Preliminary report, presented and distributed on September 30, 2008, at the
8th International Conference on Creep and Shrinkage of Concrete
(CONCREEP-8), held in Ise-Shima, Japan
Revised March 9, 2009 (download from: *http://www.civil.northwestern.edu
/people/bazant/PDFs/Papers/PalauCreep-09-03-9.pdf*)

Explanation of Excessive Long-Time Deflections of Collapsed Record-Span Box Girder Bridge in Palau

Zdeněk P. Bažant, Guang-Hua Li, Qiang Yu,
Gary Klein and Vladimír Křístek

Preliminary Structural Engineering Report
No. 08-09/A222e

Infrastructure Technology Institute
McCormick School of Engineering and Applied Science
Northwestern University
Evanston, Illinois 60208, USA

September 19, 2008
Updated March 9, 2009

Explanation of Excessive Long-Time Deflections of Collapsed Record-Span Box Girder Bridge in Palau[1]

Zdeněk P. Bažant[2], Guang-Hua Li[3], Qiang Yu[4], Gary Klein[5] and Vladimír Křístek[6]

Abstract: Explanation of the excessive deflections of the Koror-Babeldaob (KB) Bridge in Palau is presented. This bridge was built in 1977 by the cantilever method and collapsed 3 months after remedial prestressing in 1996. It was a segmental prestressed concrete girder having the world-record span of 241 m (790 ft.) and maximum girder depth of 14.17 m (46.5 ft). The final mid-span deflection was in design expected to be 0.55 to 0.67 m (21.6 to 26.4 in), but after 18 years it reached 1.39 m (54.6 in.) and was still growing. Presented is a comprehensive analysis using 5906 three-dimensional (3D) finite elements and step-by-step integration in time. For the concrete creep and shrinkage properties, the B3, GL, ACI and CEB (or CEB-FIP, fib) models are considered and predictions compared. Model B3, in contrast to the others, does not give an unambiguous prediction because, in addition to concrete design strength, it necessitates further input parameters which are unknown. These are three mix parameters which can be set to default values but can also be varied over a realistic range to ascertain the range of realistic predictions. The findings are as follows: 1) For model B3, one can find plausible values of input parameters for which all the measured deflections (as well as Troxell et al.'s 23-year creep tests) can be closely matched, while for the other models they cannot even be approached and the observed shape of creep curve cannot be reproduced. 2) The 19-year deflections calculated by 3D finite elements according the ACI, CEB and GL models are about 67%, 62% and 54% less, respectively, than those measured and calculated according to model B3, and their deflection curves have shapes rather different from the those measured. 3) The shear lag is important since it increases the downward deflection due to self-weight much more than the upward deflection due to prestress. 4) The deflection is highly sensitive to prestress loss because it represents a small difference of two large numbers (deflections due to self-weight, and to prestress). According to the ACI, CEB and GL models, the prestress loss obtained by the same finite element code is, respectively, about 54%, 44% and 34% smaller, and according to the classical lump estimate used in design about 54% smaller. 5) Model B3 is in agreement with the measurements if 3D finite elements with step-by-step time integration are used to calculate both the deflections and the prestress losses, and if the differences in shrinkage and drying creep properties caused by differences in slab thickness and temperature are taken into account.

Introduction

The Koror-Babeldaob (KB) Bridge connected the islands of Koror and Babeldaob in the Republic of Palau in tropical Western Pacific (Fig. 1a). When completed in 1977, the 241 m (790

[1]March 2009 revision of September 2008 original version, prepared after additional data were obtained and more accurate calculations were completed. Also, Appendix III on Japanese bridges is added

[2]McCormick Institute Professor and W.P. Murphy Professor of Civil Engineering and Materials Science, Northwestern University, 2145 Sheridan Road, CEE/A135, Evanston, Illinois 60208; z-bazant@northwestern.edu.

[3]Graduate Research Assistant and Doctoral Candidate, Northwestern University.

[4]Post-doctoral Research Associate, Northwestern University.

[5]Principal, Wiss, Janey, Elstner, Inc., 330 Pfingsten Rd., Northbrook, Illinois 60062-2095.

[6]Professor, Faculty of Civil Engineering, Czech Technical University in Prague, Czech Republic.

ft.) main span set the world record for prestressed concrete box girder bridges[1]. The final deflection was expected to terminate at 0.55 to 0.67 m (21.6 to 26.4 in.), according to the original CEB-FIP design recommendations (1970-72[2]), which were used in design[3,4]. According to the 1972 ACI model[5], which has been in force until today, the deflection would have been predicted as 0.71 m (28 in.)[6]. Unfortunately, after 18 years, the deflection, measured since the end of construction, reached 1.39 m (54.6 in.) and kept growing[3,7]. Compared to the design level, the mid-span sag was 0.076 m higher, i.e., 1.47 m because not all of the camber planned to offset future deflections could be introduced. Remedial prestressing was undertaken, but 3 months after its completion (on September 26, 1996) the bridge suddenly collapsed into the Toegel channel, with two fatalities (Fig. 1b)[6,8–12].

As a result of legal litigation, the data collected on this major catastrophe by the investigating agencies have been sealed and unavailable for many years. However, on November 6, 2007, the 3rd Structural Engineers' World Congress in Bangalore endorsed a resolution (proposed by the first writer, with the support of many experts). The resolution, which was circulated to major engineering societies, called, on the grounds of engineering ethics, for the release of all the technical data necessary for analyzing major structural collapses, including the bridge in Palau (see Appendix II). Subsequently, the Attorney General of Palau gave his permission.

The objective of this article is to explain the reasons for the excessive long-term deflections and draw lessons for the creep and shrinkage analysis of structures. Analysis of the remedial measures and the direct causes of collapse is planned for a forthcoming separate article.

Research Significance

Clarification of the causes of major disasters has been, and will always be, the main route to progress in structural engineering. Understanding of the excessive deflections of the bridge in Palau has the potential of greatly improving the predictions of creep and shrinkage effects in bridges as well as other structures. It may also help to resolve the currently intractable disagreements in technical committees about the optimal prediction model for a standard guide.

Bridge Description and Input Data of Analysis

The main span of 241 m (790 ft.) consisted of two symmetric concrete cantilevers connected at mid-span by a horizontally sliding hinge. Each cantilever was made of 25 cast-in-place segments of depths varying from 14.17 m (46.5 ft.) at the main piers to 3.66 m (12 ft.) at mid-span. The main span was flanked by 72.2 m (237 ft.) long end spans in which the box girder was partially filled with rock ballast to balance the moment at the main pier. The total length of the bridge was 386 m (1265 ft.). The thickness of the top slab ranged from 432 mm (17 in.) at the main piers to 280 mm (11 in.) at the mid-span. The thickness of the bottom slab varied from 1153 mm (45.4 in.) at the main piers to 178 mm (7 in.) at the mid-span. The webs had an unusually small thickness of 356 mm (14 in.) in the main span. The elevation and several typical cross sections are shown in Fig. 2. Both symmetric halves of the bridge were constructed simultaneously[1,6]. The whole bridge was completed within 2 years.

According to the design, the initial total longitudinal prestressing force above the main pier was 211 MN (47,400 kips), and was provided by 316 parallel high-strength threaded bars of diameter 32.8 mm (1.25 in.) and strength 1034 MPa (150 ksi)[1,6,10] (the jacking force of each bar was 135 kips).

The mass density of concrete was $\rho = 2325$ kg/m^3 (144 lb/ft.^{3})[3]. Top slab was covered by

concrete pavement of average thickness of 76 mm (3 in.). The aggregate was crushed basalt rock of maximum aggregate size about 19 mm (3/4 in.), supplied from a quarry on the island of Malakal.

The bars (in ducts of diameter 47.6 mm or 1.875 in., later injected by grout) were placed in up to four layers within the top slab. Extended by couplers and anchored near the abutment, the prestressing bars had the diameter of 32.8 mm (1.25 in.) and ran continuously up to the segment of the main span at which the threaded ends were anchored by nuts (using the Dywidag system[13]). From the fact that the erection took about 6 month[1], it is inferred that each fresh front segment was about 7 days old when prestressed. Some tendons were stressed from one end, some from both[1,6]. Threaded bars, of diameter 32.8 mm (1.25 in.) and length 9.14 m (30 ft.) were used to provide vertical prestress of the webs (spacing from 0.3 to 3 m or 1 to 10 ft.[4]) and horizontal transverse prestress of the top slab (typical spacing is 0.56 m or 22 in.)[3,6]. The Young's modulus of prestressing steel was assumed as 200 GPa, and Poisson's ratio as 0.3. In post-collapse examination, neither the prestressed nor the unprestressed steel showed any signs of corrosion, despite the tropical marine environment.

Although the bridge design and construction were very efficient, the box girder was built with an unintended initial sag of about 290 mm (11.4 in.) at mid-span. The reason was that the camber required to offset the anticipated long-time deflections was not met during segmental erection because it would have required abrupt large slope changes[4]. This initial sag is not a deflection due to creep, and so is not included in the deflection measurements and present calculations. It means, though, that the mid-span sag corresponding to the last measured deflection was 1.47 m (57.7 in.).

The initial deflections for the first two years were benign. However, the longer-term deflections came as a surprise. In 1990, the mid-span deflection reached 1.22 m (48 in.)[14], which caused ride discomfort, vibrations after each vehicle passage, and excessive deterioration of road surface. By 1993[3], it reached 1.32 m (52 in.). In 1995, just before the roadway pavement (of average thickness of 76 mm, or 3 in.) was removed for retrofit, the mid-span deflection reached 1.39 m (54.6 in.), and was still growing[7].

Method of Creep and Shrinkage Analysis of Box Girder

As an adequate approximation under service conditions, concrete can be assumed to follow aging linear viscoelasticity with corrections for tensile cracking and nonuniform shrinkage, drying creep or Pickett effect, and temperature. The concrete deformation is then fully characterized by one of the existing models for the shrinkage strain and the compliance function $J(t, t')$ (which defines the strain at age t caused by a unit sustained uniaxial stress applied at age t'). The three-dimensional (3D) generalization is obtained assuming material isotropy, characterized by a time-independent Poisson ratio ν[15–17] ($\nu = 0.21$ was used, based on core sample tests[7]). Linear viscoelasticity implies the principle of superposition in time, whose direct application gives the stress-strain relation in the form of a history integral. However, for the sake of large-scale computer analysis, it is advantageous to avoid computation of history integrals. This is made possible by converting the compliance function to an equivalent rate-type form, which was based on the Kelvin chain model.

The long-time deflections were analyzed by three-dimensional finite elements, essential for capturing the shear lag effects, especially their different magnitudes for self-weight and prestress. The structural creep problem can be reduced to a sequence of finite element analyses for an elastic stress-strain relation with inelastic strain, one analysis for each time step (an approach

proposed in 1966[18]). Each such analysis can be carried out with a commercial finite element program. So one merely needs to write a simple driver program calling the commercial finite element program in each time step. The software ABAQUS has been chosen, and various supplemental computer subroutines have been developed to introduce the incremental effects of creep and shrinkage.

The plates of the cross section were subdivided into 8-node isoparametric elements extending through the whole thickness of the plate (slab of web). Because of symmetry, only one half of the bridge was analyzed. Together with the pier, it was subdivided into 5036 hexahedral elements. ABAQUS was used to generate the 3D mesh shown in Fig. 3. The different ages, the sequential prestressing at various times and the different step-wise load applications in the individual segments were taken into account according to the actual cantilever erection procedure (Fig. 2).

In each of the 25 segments of the central half-span, the plate thicknesses and concrete ages were different, resulting in a different shrinkage function and different compliance function for each plate of every segment. In the case of model B3, the compliance function has a separate drying creep term, and since it applies only to the in-plane directions, different compliance functions were obtained for the in-plane and transverse directions of the plates. The drying creep term of model B3 applies only to the normal strains and causes no Poisson effect. These distinctions cannot be made for other models.

The individual prestressing bars, the number of which is 316 above the main pier, were modelled as 2-node line elements, attached to concrete at the nodes. The individual bars of unprestressed steel reinforcement were modelled similarly. Since the introduction of prestress is handled by ABAQUS automatically, it sufficed to specify the prestress values of every tendon. The tendons anchored in each segment were assumed to be prestressed 7 days after that segment was cast. As the tendons were straight, the curvature friction was nil and only the wobble friction was modelled. To do that, the initial prestress was diminished according to the length of individual tendon with an approximate wobble coefficient $\kappa = 0.0003$ /ft or 0.00098/m[19].

The stress relaxation of steel tendons was estimated according to the code formula of CEB-FIP (1990)[21], and was implemented in each time interval by means of inelastic strain increments, modelled in ABAQUS as equivalent thermal strains. The prestress losses due to sequential prestressing of tendons, and to creep and shrinkage, were automatically reproduced by ABAQUS.

The initial time steps since the bridge closing at mid-span were 0.1, 1, 10 and 100 days. After that, the time step was kept constant at 100 days up to 19 years. For the hypothetical deflection prediction up to 150 years, the subsequent time steps were 1000 days (time steps increasing in geometric progression would have been computationally more efficient but would not allow matching the times of deflection measurements).

In the case of model B3, conversion of the compliance function to a rate-type creep law is particularly easy. This can be done according to the solidification theory[22–25], in which the aging is taken into account by means of volume growth of the solidifying component, and by a gradual increase with age of the flow term viscosity. This makes it possible to use a non-aging compliance function for the solidifying component, for which one can uniquely determine a continuous retardation spectrum by a simple explicit formula (Widders's formula). The parameters of the Kelvin model are in this case constant (i.e., non-aging) and are simply obtained as a discrete representation of the continuous spectrum. The time integration utilized the exponential algorithm[25–27], which is explicit and unconditionally stable, and requires no iteration.

Despite prestress, calculations showed the top slab to get into tension after the first year. Large tensile cracks were not observed (JIAC[14], and ABAM[3] reports only sparsely located cracks in the first 6 segments from the mid-span). However, calculations that ignore the tensile strength limit f'_t revealed, for later years, tensile stresses several times larger than the f'_t. Because of this fact, due mainly to excessive prestress loss, a nonlinear tensile stress-strain relation with a tensile strength limit was implemented in ABAQUS (thanks to dense reinforcement, capable of preventing localization of cracking, cohesive crack modeling was unnecessary). The tensile strength was estimated as $\bar{f}'_t = 6\text{psi}\sqrt{\bar{f}'_c/\text{psi}} = 3.0$ MPa (433 psi).

It may be noted that core tests made before the retrofit revealed the porosity to be high and the elastic modulus to be about 21.7 GPa, which was about 33% lower than that obtained by ACI empirical formulas from the design compression strength and for the strength gain with age, which was 28.0 GPa. However, the low strength of cores was most likely a local deviation because matching of the mid-span deflection measured in the truck load test indicated the average elastic modulus of 23.5 GPa, which may be regarded as the average elastic modulus in the girder. Because of this fact, and because of uncertainty about the loading rate and time delay in the truck test, the elastic modulus of concrete inferred from the compression strength according to the ACI formula was selected for comparing the design predictions based on different models, including model B3, set 1 (defined later), while the calculations based on Model B3, set 2, used the elastic modulus calculated from the truck loading test which was made on this bridge.

As for tensile cracking, which must have taken place because of excessive prestress loss, its effect was not large, though not negligible either—the 19-year deflection with the tensile strength limit was about 3% larger than it was for unlimited tensile strength.

The pavement layer of 76 mm (3 in.) thickness, which was made of a lower quality concrete with a unit weight about 5% smaller, was doubtless heavily cracked and was not anchored against sliding over the top slab. Therefore, it was assumed incapable of resisting the applied loads.

The microprestress-solidification theory[28], which allows a more accurate representation of both drying creep and aging, would have been more realistic. However, it would have required calculating the distributions of pore relative humidity across the thickness of each slab, which would have necessitated not one but at least six finite elements over the slab thickness.

For the uniaxial compliance functions of models other than B3, the solidification theory cannot be applied. To incorporate them into the present step-by-step finite element computations, different discrete sets of spectral values of the retardation spectrum for different ages had to be calculated from the respective compliance functions and stored in advance of the finite element step-by-step analysis; see Appendix I. It was also verified that this calculation yields for model B3 the same deflection curve as the solidification theory.

Creep and Shrinkage Models Considered

The deflections were analyzed on the basis of model B3[22–25,29,30], the ACI model[31], the CEB (or CEB-FIP, fib) model[32], and the GL model of Gardner and Lockman[33,34]. The same 3D finite element analysis using ABAQUS, with Kelvin-chain based step-by-step integration in time (Appendix I), has been used for all these models.

The main material model used for the creep and shrinkage analysis was model B3, which was first presented in Ref. [29], was slightly updated in Ref. [30], and was summarized in Ref. [25]. It represented a refinement of the earlier BP and BP-KX models[35,36]. Theoretical justification

was provided in Ref. [28, 37, 38]. The B3 compliance function for basic creep was derived and experimentally supported in Ref. [22-24]. In statistically unbiased comparisons with the most complete database[39], model B3 came out as superior to other existing models[40,41].

The input parameters of creep and shrinkage prediction models are divided into extrinsic and intrinsic. For all models, the extrinsic ones are:

(1) the age at start of drying, taken as $t_0 = 7$ days, assumed equal to the segmental erection cycle (5 to 10 days)[4];

(2) the average environmental humidity $h = 0.75$;

(3) the effective thickness of cross-section $D = 2V/S$, to which a minor correction k_s for body shape is applied in the case of model B3; $k_s = 1$ for all slabs and webs considered here (notation: V/S = volume-surface ratio);

(4) for the extended model B3[25,30], also the temperature.

A correction for steam curing enters the ACI model but is not relevant here. The cement was of type I[4], which was assumed for all the models. Note that t and t' are independent variables of the compliance function and are not considered as input parameters.

The intrinsic input parameters, which reflect the composition of concrete, vary from model to model. The formulation of the ACI, CEB and GL models was driven by simplicity, as desired by many engineers. Accordingly, the only important intrinsic parameter in those models is the standard 28-day compression strength f'_c, and major influencing parameters such as the cement content and the water-cement and aggregate-cement ratios are not taken into account.

Model B3 is special in that there are more free intrinsic input parameters, which introduce the major effects of concrete composition. If unknown, these parameters allow more freedom. They can, of course, be set equal to their recommended default values. But the advantage of these free parameters is that one can explore the reasonable ranges of the unknown concrete mix parameters, run the computation of structural response for various plausible sets of values of these parameters, and thus get a picture of the possible range of structural responses to expect. This is best done statistically, as described later.

The compliance function of model B3 is separated into the basic creep part, with intrinsic parameters q_1, q_2, q_3, q_4, and the drying creep part, with intrinsic parameter q_5. The shrinkage is defined by two intrinsic parameters, the reference final shrinkage $\epsilon_{s\infty}$ and rate parameter k_t, which is proportional to $1/C_1$ or, equivalently, to $1/P_1$ where C_1 and P_1 are the reference drying diffusivity and permeability.

The best way to determine these parameters is to fit compliance data obtained experimentally in creep tests[22–24], provided that either short-time tests on the given concrete are made or previous tests of a similar concrete are available. One can also consider data for various concretes to get a picture of various possible responses to expect. The trouble with long-time prediction is that test data exceeding 3-year duration are not abundant. Those exceeding 10 years are very scant; the only ones that exist are those of Troxell (8700 days), Brooks (3650 days), and Russell and Burg (6768 days)[17,30], but are incomplete in terms of ages at loading or humidity conditions.

A simpler way, recommended in Ref. [29, 30], is to use empirical formulas estimating the intrinsic parameters from concrete composition; see Eqs. 1.16–1.23 in Ref. [30] in which q_1 is a function of elastic modulus E_c, q_2 of mean compressive strength $\bar{f}_c$ and cement content c, q_3 of water-cement ratio w/c, $\bar{f}_c$ and c, q_4 of aggregate-cement ratio a/c, $\epsilon_{s\infty}$ of $\bar{f}_c$ and water content w, k_t of $\bar{f}_c$ and diffusivity C_1, and q_5 of $\bar{f}_c$ and $\epsilon_{s\infty}$. These formulas were calibrated by numerous data for the first few years of creep, and the parameters depending on multi-year tests could not be properly experimentally validated because of data scarcity. This problem

particularly afflicts the formulas for q_3 (the non-aging viscoelastic term) and q_4 (the flow term), because they govern mainly the long-time creep.

Two sets of input parameters have been considered in computations:

Set 1: For the simple prediction on the basis of concrete composition, the following input has been used:

(1) the mean compressive strength at 28 days, which is the only relatively certain input parameter for the KB Bridge; it was estimated as $f'_{cr} = 35.9$ MPa (5200 psi) from the specified design strength $f'_c = 34.5$ MPa (5000 psi)[6], under the assumption of a typical standard deviation;

(2) the 28-day elastic modulus, not known but estimated as $E_c = (57,000 \text{ psi})\sqrt{f'_{cr}/\text{psi}}$, which gives $E_c = 28.3$ GPa (4110 ksi).

(3) $c = 620$ lb/yd^3, $a/c = 3$ and $w/c = 0.62$[4].

The result was:

$$q_1 = 0.149, q_2 = 1.02, q_3 = 0.044, q_4 = 0.065, q_5 = 2.27 \qquad (10^{-6}/\text{psi}) \tag{1}$$

$$\epsilon_{k\infty} = 0.0011 \quad \text{and} \quad k_t = 16 \qquad \text{(Set 1)} \tag{2}$$

Set 2 (updated): For a better estimate, only the values of q_2, q_5 and $\epsilon_{s\infty}$, governing mainly the response for the first few years, have been estimated from the composition. To this end, empirical formulas were used while, for the remaining parameters, the values

$$q_1 = 0.185 \ (10^{-6} \ /\text{psi}), q_3 = 0.154 \ (10^{-6} \ /\text{psi}), q_4 = 0.141 \ (10^{-6} \ /\text{psi}) \qquad \text{(for Set 2)} \tag{3}$$

were identified by a trial-and-error procedure, conducted with three objectives in mind: (1) use concrete modulus measured in the truck test, (2) stay close to the values that fit the 23-year creep tests of Troxell, the 18-year tests of Russel and Burg, and 10-year tests of Brooks, and (3) obtain a close fit of the measured deflection of the KB Bridge.

According to the empirical Eqs. 1.18–1.19 in Ref. [30], the aforementioned values of q_3 and q_4 correspond to an unreasonably large w/c. This must be seen not as a shortcoming of the present analysis but as a shortcoming of Eqs. 1.18–1.19 themselves. For long-times, these empirical equations of model B3 will eventually have to be revised. Due to extreme scarcity of long-time data, the way to do that would be the inverse analysis of measured long-term deflections of various bridges, similar to the present analysis.

A problem has been that, to calculate and compare true predictions of various models, all the properties of concrete and environmental histories of the KB Bridge concrete would have to be known, and they are not. So, the predictions of various models can be compared neither with the data nor mutually. What can be compared is whether the observed deflections are within the realistic range of possible predictions of each model. As will be seen, they are for model B3, but not at all for other models which include the ACI, CEB and GL models. The predictions of these other models are essentially fixed by the value of concrete strength, with none or little other flexibility. But not for model B3, because there exist important input parameters of unknown values that are free to choose.

Calculations revealed extreme sensitivity of deflections to the differences in the rates of shrinkage and drying creep between the top and bottom slabs. Thanks to the fact that model B3 is physically based, the differences in its parameters between top and bottom can be deduced from physics, in this case from the known influence of the drying rates. These rates are characterized by the shrinkage half-times $\tau_{sh} = k_t(k_s D)^2$ (see Eq. 1.11 in Ref. [30]) where k_t can be estimated from empirical equation 2.20 in Ref. [30].

However, there also exists in model B3 a physical estimate $k_t = 0.03/C_1$ (see Eq. 28.12 in Ref. [25]) where $C_1 = k_a P_1$ = diffusivity, $k_a \approx$ constant, and P_1 = permeability of concrete, which depends on temperature and on the extent of cracking. The bottom slab probably had the mean temperature of 25 °C, but the top slab, exposed on top to intense tropical sunlight, was probably some 30 °C warmer during the day. According to the curves for the effect of temperature on permeability in Fig. 10.3 (b,c) of Ref. [42], this likely caused a 10-fold decrease of τ_{sh}. Furthermore, noting that, according to the experiments reported in Ref. [43], cracks of width 0.15 mm increase the drying rate about 3-times, one must suspect that hairline cracks developed in the top slab since it was under tension. No such crack could have developed in the bottom slab since it was always compressed. Therefore, Eq. 1.20 of Ref. [30], giving $k_t = 16$, was used only for the bottom slab and the webs, and the value $k_t = 16/30 = 0.53$ was considered for the top slab.

Model B3 predicts the basic creep of the material (i.e., the part of creep unaffected by moisture content variation) as well as the additional effects of drying. These effects consist of the average shrinkage and average drying creep (or stress-induced shrinkage) in the cross section, and depend on the effective thickness D of the cross section.

It used to be commonplace to consider one V/S value as a characteristic of the whole cross section, i.e., to take $D = 2V/S$ with V = volume and S = surface of cross-section slice of the whole box. In that case D was a property of the whole cross section, resulting in supposedly uniform shrinkage and uniform creep properties. Recently, however, it was shown [44] that, to avoid serious errors, differences in the drying rate due to different thicknesses D_i ($i = 1, 2, 3$) of the top slab, bottom slab and the webs must be taken into account.

A simple way to do that, demonstrated in Ref. [44], is to apply a model such as B3 separately to each part of the cross section. Since the drying half-times are proportional to slab-thickness-square, the thickness differences then yield different shrinkage and drying creep properties in different parts.

The data presented here include all the input parameters needed to obtain the compliance functions for the ACI, CEB and GL models. Many of these influencing parameters, however, cannot be taken into account in these models.

Some engineers consider it advantageous if the model predicts creep and shrinkage from fewer parameters, particularly from the concrete strength only. However, such a view is dubious. In a model with many parameters, the unknown ones can always be selected at their typical, or default, values, and some predictions can still be made even if only the strength is known. But the presence of all relevant influencing parameters in model B3 makes it possible to explore the range of responses to expect, and design the structure for the most unfavorable realistic combination. With the other models this is impossible.

As it transpired from recent research [37], the other models considered here have some serious deficiencies, theoretical as well as practical. One of them, especially for the ACI model, is that the long-time creep is strongly underestimated. Another deficiency of the ACI model, and to a lesser extent the CEB model, is that the drying creep, which is sensitive to thickness, is not separated from the basic creep, and that the effects of cross section stiffness on shrinkage and drying creep are given by a scaling factor rather then as a delay.

According to the ACI model, an increase in thickness reduces creep and shrinkage through a certain constant multiplicative factor and scales down the final value for infinite time. In reality, though, an increase in thickness does not change the final value (except for a small indirect effect due to affecting the final degree of hydration). Rather, it causes a delay, properly modelled as an increase of the shrinkage half-time proportional to the thickness square (e.g., if

the ultimate shrinkage of a slab 0.10 m thick is reached in 10 years, for a slab 1 m thick it is reached in 1000 years, i.e., virtually never).

Calculated Deflections and Prestress Loss, and Comparisons to Measurements

As a first check of the finite element code, comparison was made with the bridge stiffness, which was measured in January 1990 by Japan International Cooperation Agency (JICA). A downward deflection of 0.10 ft. (30.5 mm) was recorded at mid-span when two 12.5 ton trucks were parked on each side of the mid-span hinge (one previous paper erroneously assumed that only one truck was on each side). The finite element code based on model B3 predicted the deflection of 0.098 ft. (30 mm) under the load of 250 kN that was applied gradually within 2.4 hours. Given the uncertainty about the actual rate of loading, the difference is small enough.

The results of calculations are shown in figures 4–8, both in linear and logarithmic time scales (t = time measured from the start of construction, and t_1 = duration of the construction). The data points show the measured values. The solid diamonds represent the data reported by the firm investigating the collapse[7], and the solid circles the data accepted from a secondary source[14]. For comparison, the figures show the results obtained with model B3 and the ACI, CEB and GL models. All these responses have been computed with the same finite element program and the same step-by-step time integration algorithm, in which the different thicknesses of the slabs and webs were considered. The response of the GL model is also shown for the total deflection curve (Fig. 4 and Fig. 5).

Fig. 4 shows the deflection curves up to the moment of retrofit at about 19 years of age. Since well designed bridges (such as the Brooklyn Bridge) have lasted much longer, Fig. 5 shows the same curves extended up to 150 years under the assumption that there has been no retrofit and no collapse.

Figures 7–8 clarify the mid-span deflection and prestress loss obtained (1) if the drying creep is neglected, (2) if both the shrinkage and drying creep are neglected, and (3) if the creep and shrinkage properties are considered to be uniform over the cross section, based on the effective thickness $D = 2V/S$ for the whole cross section. Note that the use of uniform creep and shrinkage properties throughout the cross section neglects the effects of differential shrinkage and differential drying creep and gives results very close to those for basic creep alone.

Accuracy in calculating the prestress loss is essential because the bridge deflection is a small difference of two large but uncertain numbers—the downward deflection due to self-weight, and the upward deflection due to prestress. For the sake of illustration, compared to the classical theory of bending, the shear lag increased the elastic downward deflection due to self-weight by 18%, and the elastic upward deflection due to initial prestress by 14%, and the total deflection by 30%.

The measured 18-year deflection, which was 1.39 m, is matched by the deflection calculated from model B3 (set 2). This measured deflection is about 3-times larger than those calculated for the ACI, CEB (which are 0.47 m and 0.53 m), and about the double of that from the GL model (which is 0.65 m); see Fig. 4. Besides, the ACI, CEB and GL deflection curves have shapes rather different from model B3. They give too much deflection during the first year, and far too little from 3 years on, especially for the ACI and CEB models. An important point to note is that the 18-year prestress loss is less than 30% when the ACI and CEB models are used in the present three-dimensional finite element calculations, but about 46% when model B3 is used (Fig. 6).

Table 1: Summary of strain relief tests on the KB Bridge in Palau

Tendon	Location	Gage		Initial			Final			Δ ($\mu\epsilon$)	σ (psi)
1	1	500	500	503	504	503	339	340	340	1637	47463
	2	500	500	533	532	533	368	368	368	1647	47753
	3	500	500	529	530	531	361	360	360	1697	49203
	average										48140
2	4	500	500	558	558	556	377	376	377	1807	52393
	5	500	500	532	532	532	351	352	353	1800	52200
	6	500	500	531	531	531	353	352	352	1787	51831
	average										52136
3	7	500	500	511	510	510	286	287	288	2233	64767
	8	500	500	466	466	465	244	244	244	2217	64283
	9	500	500	520	518	519	303	303	303	2163	62737
	average										63929

The correctness of B3 prestress loss is confirmed by stress relief tests which were made by ABAM on 3 tendons before the retrofit[7]. Sections of three tendons were bared, and strain gages were glued at 3 different locations on each of the three tendons (to average the readings). Each of these tendons was cut, and the stress was calculated from the gage deformation caused by the cut; see Table 1. The average stress in the tendons was thus found to be 377 MPa (54.7 ksi). This means that the actual prestress loss was about 50%[1,6,12], which is closely matched by model B3 (set 2).

If only nondestructive approach is permitted, measurement of stresses in grouted tendons is next to impossible. Thus the KB Bridge, in which tendon cuts were permissible since additional tendons had to be installed anyway, provided a unique opportunity to learn about the actual stresses in tendons.

In the mid 1970s, the prestress loss was calculated not by finite elements but by simple formulas based on the beam theory[19]. A lump estimate of the final prestress loss was generally used and, according to Ref. [4], it was used for the KB Bridge. According to p. 257 of Ref. [19], this estimate would have been 23%, which is marked in Fig. 6 by a horizontal dashed line. The error compared to the prestress measured before retrofit and the present calculation is enormous. This error is one reason why the long-time deflections were so badly underestimated in design.

One must conclude that, for large box girders, the standard textbook formulas for prestress loss are inadequate and dangerously misleading.

The final downward slope of the deflection curve in the logarithmic time scale (Fig. 4), obtained from both the measurements and the calculations based on model B3, is quite high, while for the ACI and CEB models it is nearly zero. The long-time deflections are seen to evolve almost linearly in the logarithmic scale (which is to be expected for theoretical reasons[37]), and can thus be extrapolated to longer times graphically; see Fig. 5. The straight-line extrapolation is seen to agree almost exactly with model B3 calculation up to 150 years. Note that, if the bridge were left standing without any retrofit, the 150-year deflection would have reached 2.24 m (7.35 ft.).

The main reason for the large effect of thickness difference between the top and bottom slabs on the early deflections and the early prestress loss is the differential shrinkage and the

difference in the drying creep compliance between the top and bottom slabs. In a previous study of the effect of thickness difference between the top and bottom slabs on deflections[44], the effect of differential drying creep was found to be small in comparison to the effect of differential shrinkage. Here the difference in drying creep compliance is almost as important as the differential shrinkage. The reason is that initially the prestress in the top slab is high enough to cause a high drying creep.

A typical feature of prestressed box girders erected as segmental cantilevers is that initially, during the first 1 month to 3 years, the deflections are negative, i.e., upwards[44]. Measurements to confirm this behavior for the KB Bridge are unavailable. However, the present calculations support it (Fig. 4).

Altogether, one can identify four principal reasons why the measured deflections can be matched by model B3 (set 2) but not the ACI, CEB and GL models:

(1) A significantly higher long-time creep in model B3, compared to the ACI, CEB and GL models. There are three reasons for that: a) theoretical advances during the last three decades, incorporated in model B3[25,30,37]; b) model calibration by a larger database, with a rational statistical calibration procedure compensating for the database bias for short times and for small specimen sizes[39,45]; and c) adjustment of the model to the shape of creep curves observed in individual long-time tests (5 to 25 years), which is obscured when the database is only considered as a whole[31].

(2) Three-dimensional analysis of deflections and prestress loss, which is more realistic than the beam bending analysis, especially because it can capture different effects of shear lag on the downward deflection due to self-weight and the upward deflection due to prestress.

(3) Realistic representation of nonuniform shrinkage and drying creep properties in the cross sections, caused by the effect of different wall and slab thicknesses on the shrinkage and drying creep rates and half-times, as well as by the differences in permeability due to temperature differences and cracking.

(4) A larger number of input parameters in model B3, which include the water-cement ratio and aggregate-cement ratio. This allows a greater range of responses to be explored in design, compared to the ACI, CEB and CL models. These models are inflexible because of missing these input parameters, and thus provide a unique response if the strength of concrete is fixed.

Uncertainty of Deflection Predictions and Calculation of Confidence Limits

Creep and shrinkage are notorious for their relatively high random scatter. For this reason, it has been argued for the last two decades that the design should be made not for the mean deflections, but for some suitable confidence limits such as 95%[40,46]. Adopting the Latin hypercube sampling of input parameters[46], one can easily obtain such confidence limits by repeating the deterministic computer analysis of the bridge 8-times, one run for each of 8 different randomly generated samples of 8 input parameters.

The range of the cumulative distribution of each random input variable (assumed to be Gaussian) is partitioned into N intervals of equal probability. The parameter values corresponding to the centroids of these intervals are selected according to randomly generated Latin hypercube tables (which can be freely downloaded from the ITI website–http://iti.northwestern.edu/generator, so that a bridge designer would not need to work with a random number generator at all). The values from the rows of these tables are then used as the input parameter for N deterministic computer runs of creep and shrinkage analysis.

By experience, it is sufficient to chose $N = n =$ number of random input parameters (here $N = n = 8$). One random input variable is the environmental relative humidity h, whose mean and coefficient of variation are estimated as 0.75 and 0.2 (or 75% and 20%). The others are the material characteristics $q_1, q_2, q_3, q_4, q_5, k_t$ and ϵ_∞, representing the parameters of model B3. According to model B3, the means of these parameters for the KB Bridge are found to be: $q_1 = 0.185$, $q_2 = 0.102$, $q_3 = 0.132$, $q_4 = 0.141$, $q_5 = 2.27$, $k_t = 16.05$, and $\epsilon_\infty = 0.0011$. The estimated coefficient of variation is 23% for creep parameters q_1, q_2, q_5 and 30% for q_3, q_4 (which is higher because of uncertainty and scarcity of long-term creep data), and 34% for shrinkage parameters $k_t = 16$ and ϵ_∞.

The responses from each deterministic computer run for model B3 (set 2), particularly the mid-span deflections at specified times, are collected in one histogram of 8 values, whose mean $\bar{w}$ and coefficient of variation ω_w are the desired statistics. Knowing these, and assuming the Gaussian (or normal) distribution, one can get the one-sided 95% confidence limit as $w_{95} = \bar{w}(1 + 1.645\omega_w)$ (which is exceeded with the probability of 5%; in other words, one out of 20 identical bridges would exceed that limit, which seems to give optimal balance between risk and cost).

The curves of the mean, and of the one-sided 95% and 5% confidence limit for the KB Bridge in Palau, are shown (for model B3, set 2) in Fig. 9. Note that the curves of the present finite element calculations according to the ACI and CEB models lie way outside the statistical confidence band obtained with model B3 (and the traditional prediction lies even farther).

The probabilistic problem of deflections is fortunately much simpler than that of structural safety. For the latter, the extreme value statistical theory must be used since the tolerable probability of failure is $< 10^{-6}$, far less than the value of 0.05 acceptable for deflections.

Comparison with Analysis by Bending Theory with Plane Cross Sections

Traditionally, box girders have been analyzed according to the classical engineering theory of bending in which the cross sections are assumed to remain plane. However this engineering theory of bending is too simplified to capture the deformation of box girders accurately. Its main deficiency is that it lacks the effect of shear lag, both in the top slab and in the web, and both for self weight and for prestress. In Fig. 10, the distribution of shear stress in a cross section located at 7.08 m (23.3 ft.) away from main pier face, is shown when only self weight or only prestress is considered. It can be seen that a significant shear stress exists in the top and bottom slabs.

The total deflection is sensitive because it represents a small difference of two large numbers corresponding to self weight and to prestress. The shear lag plays a more important role in downward deflection by self weight than upward deflection by prestress. Therefore the neglect of shear lag may lead to a considerable underestimation of the long-term deflection.

The significant discrepancy between full 3D simulation and engineering theory of bending is demonstrated in Fig. 11. The deflections and prestress losses obtained in this classical way for B3, ACI, CEB and GL models are compared with 3D analysis. A large error, which is about 30% less in long-term deflection, is found for this classical engineering approach.

In the KB Bridge design, an approximate correction for the shear lag in the top slab due to self weight was introduced[4] through the classical effective width concept[47–51]. For total deflections, however, this classical concept can still give major errors compared to the full 3D analysis.

Causes of Excessive Deflections and Lessons Learned

As confirmed by this study, the following ten points are essential for correctly predicting the long-time response of bridges highly sensitive to creep and shrinkage.

1. The 1972 ACI model (reapproved in 2007[31]), and to a lesser extent the CEB model, are obsolete. They severely underestimate the long-time deflections as well as the prestress losses, for a number of reasons[37]. They lack a solid theoretical foundation, do not reflect the theoretical advances of the last three decades[37], and have not been experimentally calibrated by a large and complete database[30] using a sound statistical method[39,45] offsetting statistical bias. The recent GL model gives better predictions, but not sufficiently better (its long-term creep is too low, the model does not have enough intrinsic input parameters, the effect of temperature and cracking on diffusivity cannot be accounted for, etc.)

2. The effect of thickness differences among the webs and top and bottom slabs on shrinkage and drying creep must be taken into account. This leads to non-uniform creep and shrinkage properties throughout the cross section, manifested as differential drying creep and differential shrinkage.

3. Because of its thickness dependence, the drying creep should be separated in the prediction model from the basic creep, which is independent of thickness. As evidenced by the KB Bridge, the thickness-induced differences in the compliance functions for drying creep can be as important as those in shrinkage.

4. The effect of slab or web thicknesses on the drying creep rate and the shrinkage rate must be taken into account. This means that the half-time of shrinkage and drying creep should be proportional to the thickness square and their curves should initially evolve as a square root of time (as dictated by the diffusion theory[37]). Further it is appropriate to take into account the effect of temperature differences on the drying rates.

5. The prestress loss may be 2- to 3-times higher than predicted by simple textbook formulas or lump estimates. It can also be much higher than that predicted by the theory of beam bending in which the cross sections remain plane. The loss should be calculated as part of 3D finite element analysis, using a sound creep and shrinkage model and taking into account the nonuniformity of shrinkage and drying creep properties throughout the cross section.

6. The main reason why a 3D analysis is necessary is that it automatically captures the effect of shear lag, as well as the effects of differential shrinkage and drying creep. The neglect of shear lag, which causes a nonlinear distribution of normal stresses over the slabs and the webs within the cross section, leads to underestimation of deflections and prestress losses.

7. The shear lag effects on deflections due to self weight and to prestress are different. The self weight produces large vertical shear forces in the web at the piers, but the prestress does not. Thus the shear lag is strong for the self weight but weaker for the prestress. Since the total deflection is a small difference of two large numbers, one for the downward deflection due to self-weight and the other for the upward deflection due to prestress, a small percentage error in the first, typically 10% to 15%, will result in a far larger percentage error in the total deflection.

8. When dealing with large creep-sensitive structures, updating of the creep and shrinkage prediction based on short-time tests of the given concrete is necessary. However, even when short-time tests were made for some structures in the past, their conduct has usually been incorrect. Previous research showed that an order-of-magnitude error reduction in the long-time creep and shrinkage predictions can be achieved with model B3 by means of updating on the basis of one-month creep and shrinkage tests of the particular concrete to be used, provided that they are accompanied by water loss measurements [30]. Such tests were not made for the KB Bridge, but have met with success for some recent large bridges [52]. B3 is a model that has been specifically formulated so as to allow easy updating by linear regression, while for other models the updating problem is nonlinear.

9. Large bridges should be designed not for the mean but for 95% confidence limit on the predicted deflection (in other words, having to repair or close more than 1 bridge in 20 is unacceptable). The necessary statistical analysis is easy. It suffices to repeat a deterministic computer run of structural response about ten-times, using properly selected random samples of the input parameters. Then one needs to evaluate the mean and variance of the calculated response values. Assuming a normal distribution, one has its both parameters, and from a table of normal distribution the confidence limit then follows.

10. As observed in Ref. [44], the deflection evolution of large box girders is usually counterintuitive. The deflections grow slowly or are even negative during the first months or years, which often leads to unwarranted optimism. Later, unfortunately, a rapid and excessive deflection growth sets in. The early deflections of the KB bridge were not measured, but according to the present calculations the bridge must have been deflecting upward for an initial period of up to 2 months (Fig. 4).

Closing Comments

If the models and methods available today were used at the time of design, the observed deflections of the KB Bridge in Palau would have been expected. This would have forced a radical change of design of this bridge.

The results obtained for the ACI model [5,31,54] (Figs. 4–6) document that this model can lead to dangerous underprediction of deflections and prestress losses. Yet this ACI model, first introduced in 1972, has recently been reapproved by ACI and is featured as one of the recommended models in ACI Guide 209.2R-08 [31] (the appearance of the first writer's name on the list of the authoring committee was mandatory and did not imply his endorsement of this Guide). Similar though milder objections apply to the CEB and GL models.

The experience with the KB Bridge and the present analysis confirms computationally the previous experience that bridges with a sliding hinge at mid-span are too vulnerable and should be avoided. Continuous box girders give significantly smaller deflections. It is worth noting that the Brooklyn bridge (span 486 m, built in 1883) and the Firth-of-Forth Bridge (span 510 m, built in 1890), which both held world records, are still in service today. In view of Fig. 5, nothing close to such a lifespan can be expected for the large prestressed concrete box girders which were designed using simple material models and simplified methods of analysis.

Designs that mitigate deflections should be sought. Continuous box girders deflect significantly less than those with a hinge at mid-span, as is already well known. In continuous girders, the deflections are particularly sensitive to tendon layout [53] and can be reduced by the right

layout. A layout benefiting the stress state can at the same time be harmful from the deflection viewpoint.

Insufficient efforts have, unfortunately, been made in the past to transfer the results of experimental and theoretical research on creep and shrinkage into practice. At the same time, these results have unjustly been regarded by many practitioners as irrelevant and artificially complex academic exercises. Many of the causes of excessive deflections of the KB bridge were in principle known from research papers already in the early 1970s [47–51,55–67]; they included the shear lag effect, the true effect of slab thickness on the drying-induced strains, the use of time curves that underpredict the long-term creep and ignore the long-time experimental data [60], and accurate step-by-step time integration of structural concrete creep problems by the exponential algorithm. The analysis of these causes was not impossible in the early 1970s, however, nobody at that time realized their importance, and even if someone did, a supercomputer of those times would have been required.

Acknowledgment. *Financial support from the U.S. Department of Transportation through Grant 0740-357-A222 from the Infrastructure Technology Institute of Northwestern University, is gratefully appreciated. Thanks are due to Dr. Khaled Shawwaf of DSI, Inc., Bolingbrook, Illinois, for providing valuable information on the analysis, design and investigations of this record-setting bridge.*

Appendix I. Simpler Variant of Step-by-Step Creep Structural Analysis for Empirical Compliance Function

Accurate and efficient creep analysis requires replacing the constitutive law with a history integral based on the principle of superposition by a rate-type creep law with internal variables based on the viscoelastic Kelvin chain model [15–17,25]. The rate-type creep formulation is particularly simple for the solidification theory underlying model B3 because the creep properties can be specified by the non-aging properties of the hardening constituent whose volume growth accounts for aging, which means that the spectrum of elastic moduli of the Kelvin chain units is constant in time and can be identified by an explicit formula from the compliance curve.

A method that simplifies programming at the expense of letting more data and more computations to be handled by the computer has now been devised. In numerical step-by-step structural analysis, the retardation spectrum is needed only for the discrete ages of concrete corresponding to the middle of the chosen time steps (for the KB bridge, 10 time steps increasing in geometric progression were used to obtain the solution up to 19 years, and 15 steps up to 150 years).

For empirical models such as those of ACI, CEB and GL, the creep analysis is more complicated since a non-aging constituent corresponding to the solidification theory cannot be identified for these models. Therefore, compliance curves that change with the age at loading must be used.

Such a situation was handled in the 1970s by considering the retardation (or relaxation) spectrum, to be age dependent, which meant that the spectrum of elastic moduli of the Kelvin (or Maxwell) chain model to be considered as age-dependent [15–17]. Identification of these moduli as functions of age was not unambiguous.

For the loading age corresponding to each time step, the ACI, CEB or GL model gives one compliance curve (or unit creep curve), for which the continuous retardation spectrum can be obtained by Widder' explicit formula for inversion of Laplace transform [68]. This continuous

retardation spectrum is then approximated by a set of discrete spectral values D_i, one set for each time step. These spectral values are then used in the individual time steps of the exponential algorithm based on Kelvin chain (as described in Ref. [15-17]). No continuous function for $D_i(t)$, which complicated the previous practice, need be identified and used.

Appendix II: Resolution of 3rd Structural Engineers World Congress on Data Disclosure Ethics

In Bangalore, India, on November 6, 2007, this Congress adopted the following resolution:

1. *The structural engineers gathered at their 3rd World Congress deplore the fact the technical data on the collapses of various large structures, including the Koror-Babeldaob Bridge in Palau, have been sealed as a result of legal litigation.*

2. *They believe that the release of all such data would likely lead to progress in structural engineering and possibly prevent further collapses of large concrete structures.*

3. *In the name of engineering ethics, they call for the immediate release of all such data.*

This resolution was proposed at the congress by Z.P. Bažant, in the name of the following group of experts whose support has been solicited in advance: P. Marti (ETH), F.J. Ulm (MIT), A. Ingraffea (Cornell University), W. Dilger (U. of Calgary), P. Gambarova, L. Cedolin, G. Maier (Politecnico di Milano), E. Fairbairn (Rio de Janeiro), W. Gerstle (U. of New Mexico), K. Willam (UC Boulder), V. Kristek (CVUT Prague), T.P. Chang (Taipei) J.C. Chern (Taipei), T. Tanabe (Nagoya), C. Leung (HKUST, Hong Kong), M. Jirasek (CVUT Prague), D. Novak, M. Vorechovsky (VUT Brno), M. Kazemi (Tehran), Susanto Teng (Singapore), R. Eligehausen, J. Ozbolt (Stuttgart U.), B. Schrefler, C. Majorana (U. of Padua), Zongjin Li (HKUST, Hong Kong), K. Maekawa (U. of Tokyo), C. Videla (Santiago), J.G. Rots (Delft), S. Teng (Singapore), H. Mihashi (Sendai), H. Mang (Vienna), B. Raghu-Prasad (Bangalore), N. Bicanic (Glasgow), I. Robertson (Honolulu), J. van Mier (Zurich), Z.J. Li (Hong-Kong), K. Maekawa (Tokyo), V. Saouma (Boulder), Y. Xi (Boulder), L. Belarbi (Missouri), L. Elfgren (Lulea), C. Andrade (Madrid), I. Carol (Barcelona), D.M. Frangopol (Lehigh), J.W. Ju (Los Angeles), T. Tsubaki (Yokohama), N.M. Hawkins (Seattle), J.-K. Kim (Korea), A. Zingoni (Cape Town).

Appendix III: Similar Excessive Deflections Documented for Japanese Bridges

Dr. Yasumitsu Watanabe, the chief engineer of Shimizu Construction Corporation, Tokyo, documented at Concreep-8 (Ise-Shima, Japan, September 30, 2008) that many Japanese box girders also deflected far more than predicted by the traditional method based based on the JSCE design code. He graciously made available to the writers the deflection data on four monitored bridges shown in Figs. 12-15. Note the similarity to the bridge in Palau, and especially the steep increase of long-time deflections seen in the logarithmic time scale.

References

[1] Yee, A.A. (1979). "Record span box girder bridge connects Pacific Islands" *Concrete International* 1 (June), pp. 22–25.

[2] Comité euro-international du béton (CEB) (1978) *Bulletin d'Information No. N. 124/125-E*, Paris, France.

[3] ABAM Engineers Inc. (1993). *Basis for design, Koror-Babeldaob bridge repairs.*

[4] Private conversation with K., Shawwaf who was a member of the design team of KB bridge, September 18, 2008.

[5] ACI Committee 209 (1971) "Prediction of creep, shrinkage and temperature effects in concrete structures" *ACI-SP27, Designing for Effects of Creep, Shrinkage and Temperature*, Detroit, pp. 51–93.

[6] McDonald, B., Saraf, V., and Ross, B. (2003). "A spectacular collapse: The Koro-Babeldaob (Palau) balanced cantilever prestressed, post-tensioned bridge" *The Indian Constrete Journal* Vol. 77, No.3, March 2003, pp. 955–962.

[7] Berger/ABAM Engineers Inc. (1996). *KB Bridge modifications and repairs.*

[8] SSFM Engineers, Inc. (1996) *Preliminary Assessment of Korror-Babeldaob Bridge Failure*, prepared for US Army Corps of Engineers, October 2, 1996.

[9] Parker, D. (1996). "Tropical Overload", *New Civil Engineer*, December 5, 1996.

[10] Pilz, M. (1997). *The collapse of the KB bridge in 1996*, Dissertation, Imperial College London.

[11] Pilz, M. (1999). "Untersuchungen zum Einsturzder KB Brücke in Palau", *Beton- und Stahlbetonbau*, May 1999, 94/5.

[12] Burgoyne, C. and Scantlebury, R. (2006). "Why did Palau bridge collapse?" *The Structural Engineer*, pp. 30-37.

[13] ABAM Engineers Inc. (1993). *Record of telephone conversation*, Aug. 13, 1993.

[14] Japan International Cooperation Agency (1990). *Present Condition Survey of the Koror-Babelthuap Bridge*, Feburary, 1990.

[15] Bažant, Z.P. (1975)."Theory of creep and shrinkage in concrete structures: A precise of recent developments" *Mechanics Today*, ed. by S. Nemat-Nasser (Am. Acad. Mech.), Pergamon Press 1975, Vol. 2, pp. 1–93.

[16] Bažant, Z.P. (1982). "Mathematical models of nonlinear behavior and fracture of concrete" in *Nonlinear Numerical Analysis of Reinforced Concrete*, ed. by L. E. Schwer, Am. Soc. of Mech. Engrs., New York, 1–25.

[17] RILEM Committee TC-69 (1988). "State of the art in mathematical modeling of creep and shrinkage of concret" in *Mathematical Modeling of Creep and Shrinkage of Concrete*, ed. by Z.P. Bažant, J. Wiley, Chichester and New York, 1988, 57–215.

[18] Bažant, Z.P. (1967) "Linear creep problems solved by a succession of generalized thermoelasticity problems" *Acta Technica ČSAV*, 12, pp. 581–594.

[19] Nilson, A.H. (1987). *Design of Prestressed Concrete*, 2nd edition, John Wiley & Sons, New York.

[20] PCI Committee (1975). "Recommendations for estimating prestress losses" *PCI Comittee Report on Prestress Losses, J. PCI*, Vol.20, No.4, July-August, pp. 43–75.

[21] *CEB-FIP Model Code 1990. Model Code for Concrete Structures.* Thomas Telford Services Ltd., London, Great Britain; also published by Comité euro-international du béton (CEB), Bulletins d'Information No. 213 and 214, Lausanne, Switzerland.

[22] Bažant, Z.P. and Prasannan, S. (1988). "Solidification theory for aging creep" *Cement and Concrete Research*, 18(6), pp. 923–932.

[23] Bažant, Z.P. and Prasannan, S. (1989). "Solidification theory for concrete creep: I. Formulation" *Journal of Engineering Mechanics ASCE*, 115(8), pp. 1691–1703.

[24] Bažant, Z.P. and Prasannan, S. (1989). "Solidification theory for concrete creep: II. Verification and application" *Journal of Engineering Mechanics ASCE*, 115(8), pp. 1704–1725.

[25] Jirásek, M. and Bažant, Z.P. (2002). *Inelastic analysis of structures*, John Wiley & Sons, London and New York.

[26] Bažant, Z.P. (1971). "Numerical solution of nonlinear creep problems with application to plates" *International Journal of Solids and Structures*, 7, pp. 83–97.

[27] Bažant, Z.P. and Wu, S.T. (1974). "Rate-type creep law of aging concrete based on Maxwell chain" *Materials and Structures* (RILEM), 7 (37), pp. 45–60.

[28] Bažant, Z.P., Hauggaard, A.B., Baweja, S. and Ulm, F.-J. (1997). "Microprestress-solidification theory for concrete creep. I. Aging and drying effects" *Journal of Engineering Mechanics, ASCE*, 123(11), pp. 1188–1194

[29] Bažant, Z.P. and Baweja, S. (1995). "Creep and shrinkage prediction model for analysis and design of concrete structures: ModelB3" Materials and Structures 28, pp. 357–367.

[30] Bažant, Z.P. and Baweja, S. (2000). "Creep and shrinkage prediction model for analysis and design of concrete structures: Model B3." *Adam Neville Symposium: Creep and Shrinkage—Structural Design Effects*, ACI SP–194, A. Al-Manaseer, ed., pp. 1–83 (update of RILEM Recommendation published in *Materials and Structures* Vol. 28, 1995, pp. 357–365, 415–430, and 488–495).

[31] ACI Committee 209 (2008). *Guide for Modeling and Calculating Shrinkage and Creep in Hardened Concrete* ACI Report 209.2R-08, Farmington Hills.

[32] FIB (1999). *Structural Concrete: Textbook on Behaviour, Design and Performance, Updated Knowledge of the of the CEB/FIP Model Code 1990.* Bulletin No. 2, Fédération internationale du béton (FIB), Lausanne, Vol. 1, pp. 35–52.

[33] Gardner, N.J. (2000). "Design provisions of shrinkage and creep of concrete" *Adam Neville Symposium: Creep and Shrinkage - Structural Design Effect* ACI SP-194, A. AlManaseer, eds., pp. 101–104.

[34] Gardner N.J. and Lockman M.J. 2001. "Design provisions for drying shrinkage and creep of normal strength" *ACI Materials Journal* 98 (2), Mar.-Apr., pp.159–167.

[35] Bažant, Z.P. and Panula, L. (1978-1979). "Practical prediction of time-dependent deformations of concrete" *Materials and Structures* (RILEM, Paris): Part I, "Shrinkage" Vol.11, 1978, pp. 307–316; Part II, "Basic creep" Vol. 11, 1978, pp. 317–328; Part III, "Drying creep" Vol. 11, 1978, pp. 415–424; Part IV, "Temperature effect on basic creep" Vol. 11, 1978, pp. 424–434.

[36] Bažant, Z.P., Kim, Joong-Koo, and Panula, L. (1991). "Improved prediction model for time-dependent deformations of concrete:" *Materials and Structures* (RILEM, Paris), Parts 1–2, Vol. 24 (1991), pp. 327–345, 409–421, Parts 3–6, Vol. 25 (1992), pp. 21–28, 84–94, 163–169, 219–223.

[37] Bažant, Z.P. (2000) "Criteria for rational prediction of creep and shrinkage of concrete" *Adam Neville Symposium: Creep and Shrinkage—Structural Design Effects*, ACI SP–194, A. Al-Manaseer, ed., Am. Concrete Institute, Farmington Hills, Michigan, 237-260.

[38] Bažant, Z.P. (2001). "Creep of concrete" *Encyclopedia of Materials: Science and Technology*, K.H.J. Buschow et al., eds. Elsevier, Amsterdam, Vol. 2C, 1797–1800.

[39] Bažant, Z.P., and Li, G.-H. (2008) "Unbiased Statistical Comparison of Creep and Shrinkage Prediction Models" *ACI Materials Journal*, (2008), in press.

[40] Bažant, Z.P., Li, G.-H. and Yu, Q. (2008) "Prediction of creep and shrinkage and their effects in concrete structures: critical appraisal" *Proc., 8th International Conference on Concrete Creep and Shrinkage* (CONCREEP-8), Ise-Shima, Japan, Oct. 2008, in press.

[41] Bažant, Z.P., Li, G.-H. and Yu, Q. (2008) "Prediction of creep and shrinkage and their effects in concrete structures: critical appraisal" Structure Engineering Report, Northwestern University, Evanston, Illinois.

[42] Bažant, Z.P. and Kaplan, M.F. (1996). Concrete at High Temperatures: Material Properties and Mathematical Models, Longman (Addison-Wesley), London (2nd printing Pearson Education, Edinburgh, 2002).

[43] Bažant, Z.P., Sener, S. and Kim, J.K. (1987). "Effect of cracking on drying permeability and diffusivity of concrete" *ACI Materials Journal*, 84, pp. 351–357.

[44] Křístek, V., Bažant, Z.P., Zich, M., and Kohoutková (2006). "Box girder deflections: Why is the initial trend deceptive?" ACI Concrete International 28 (1), 55–63. ACI SP-194, 237–260.

[45] Bažant, Z.P. and Li, G.-H. (2008). "Comprehensive database on concrete creep and shrinkage" Structure Engineering Report 02-08/A210u, Northwestern Univeristy, Evanston, Illinois.

[46] Bažant, Z.P. and Liu, K.-L. (1985). "Random creep and shrinkage in structures: Sampling" *J. of Structural Engrg. ASCE* 111, pp. 1113–1134.

[47] "Richtlinien für die Bemessung and Ausführung Massiver Brúcken". *German Standards*, Substitute for DIN 1075, Aug., 1973.

[48] Reissner, E. (1946). Analysis of Shear Lag in Box Beams by the Principle of Minimum Potential Energy" *Quart. App. Math.* 4(3), pp. 268-278.

[49] Benscoter, S.U. (1954). "A theory of Torsion Bending for Multi-cell Beams" *J. Appl. Mech. ASME*, 21(1), pp. 25-34.

[50] Abdel-Samad, S.R., Wright, R.N., and Robinson, A-R. (1968). "Analysis of Box Girders with Diaphragms". *J.Struct. Div., Proc. ASCE* 94(ST10), pp. 2231-2255.

[51] Malcolm, D.J., and Redwood, R.G. (1970). "Shear Lag in Stiffened Box Girders". *J. Struct. Div., Proc. ASCE* 96(ST7), 1403-14019, July, 1970.

[52] Navrátil (1998). "Improvement of accuracy of prediction of creep and shrinkage of concrete" (in Czech). Stavební Obzor, No. 2, pp. 44–50.

[53] Křístek, V., Vráblík, L., Bažant, Z.P., Li, Guang-Hua, and Yu, Qiang (2008). "Misprediction of long-time deflections of prestressed box girders: causes, remedies and tendon layout" *Proc., CONCREEP-8* (8th Int. Conf. on Creep, Shrinkage and Durability of Concrete, Ise-Shima, Japan), T. Tanabe, ed., Nagoya University; in press.

[54] ACI Committee 209 (1992). "Prediction of creep, shrinkage and temperature effects in concrete structures" *Report ACI 09R-92*, Detroit, March, pp. 1-12.

[55] L'Hermite, R.G. and Mamillan M. (1970). "Influence de la dimension des éprouvettes sur le retrait" *Ann. Inst. Techn. Bâtiment Trav. Publics* **23** (270) (1970), pp. 5-6.

[56] L'Hermite, R.G., Mamillan, M. and Lefèvre, C. (1965). "Nouveaux résultats de recherches sur la déformation ét la rupture du béton" *Ann. Inst. Techn. Bâtiment Trav. Publics* **18** (207-208), (1965), pp. 323-360.

[57] Mamillan, M. and Lellan, M. (1968). "Le fluage de béton" *Annalle Inst. Tech. Bat. Trav. Publics (Suppl.)* 21, No. 246, 847–850, and 23 (1970), No. 270, pp. 7–13.

[58] Rostasy, F.S., Teichen, K.-Th. and Engelke, H. (1972). "Beitrag zur Klärung des Zussammenhanges von Kriechen und Relaxation bei Normal-beton" Amtliche Forschungs-und Materialprüfungsanstalt für das Bauwesen, Heft 139 (Otto-Graf-Institut, Universität Stuttgart, (Strassenbau-und Strassenverkehrstechnik) (1972).

[59] Hansen, T.C. and Mattock, A.H. (1966). "Influence of size and shape of member on the shrinkage and creep of concrete" *ACI J.* **63**, pp. 267-290.

[60] Troxell, G.E., Raphael, J.E. and Davis, R.W. (1958). "Long-time creep and shrinkage tests of plain and reinforced concrete" *Proc. ASTM* **58** pp. 1101-1120.

[61] Browne, R.D. (1967). "Properties of concrete in reactor vessels" in *Proc. Conference on Prestressed Concrete Pressure Vessels* Group C, Institution of Civil Engineers, London, pp. 11-31.

[62] Bažant, Z.P. and Najjar, L. J. (1972). "Nonlinear water diffusion in nonsaturated concrete." *Materials and Structures* (RILEM, Paris), 5, pp. 3–20.

[63] Bažant, Z.P. (1972). "Numerical determination of long-range stress history from strain history in concrete" *Materials and Structures* (RILEM), 5, pp. 135–141.

[64] Bažant, Z.P. and Wu, S. T. (1973). "Dirichlet series creep function for aging concrete" Proc. ASCE, *J. Engrg. Mech. Div.*, 99, EM2, pp. 367–387.

[65] Harboe, E.M. et al. (1958). "A comparison of the instantaneous and the sustained modulus of elasticity of concrete" *Concrete Lab. Rep. No.* C-854, Division of Engineering Laboratories, US Dept. of the Interior, Bureau of Reclamation, Denver.

[66] Hanson, J.A. (1953). "A 10-year study of creep properties of concrete" *Concrete Lab. Rep. No.* Sp-38, Division of Engineering Laboratories, US Dept. of the Interior, Bureau of Reclamation, Denver.

[67] Weil, G. (1959). "Influence des dimensions et des tensions sur le retrait et le fluage de béton" *RILEM Bull.* No. 3, pp. 4–14.

[68] Bažant, Z.P. and Xi, Y. (1995). "Continuous retardation spectrum for solidification theory of concrete creep" *J. of Engrg. Mech.* ASCE 121 (2), pp. 281–288.

List of Figures

a)

b)

Fig. 1

Elevation

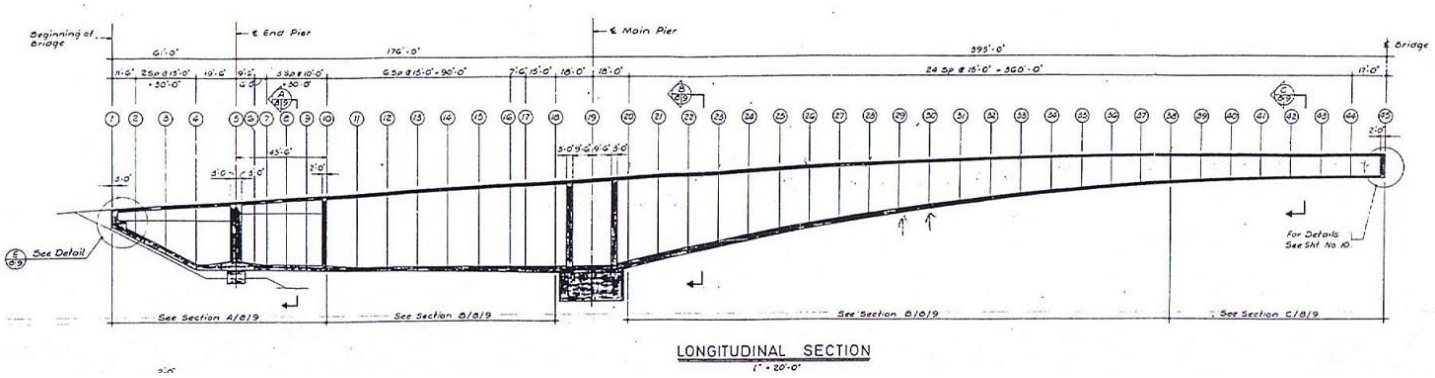

Cross-section

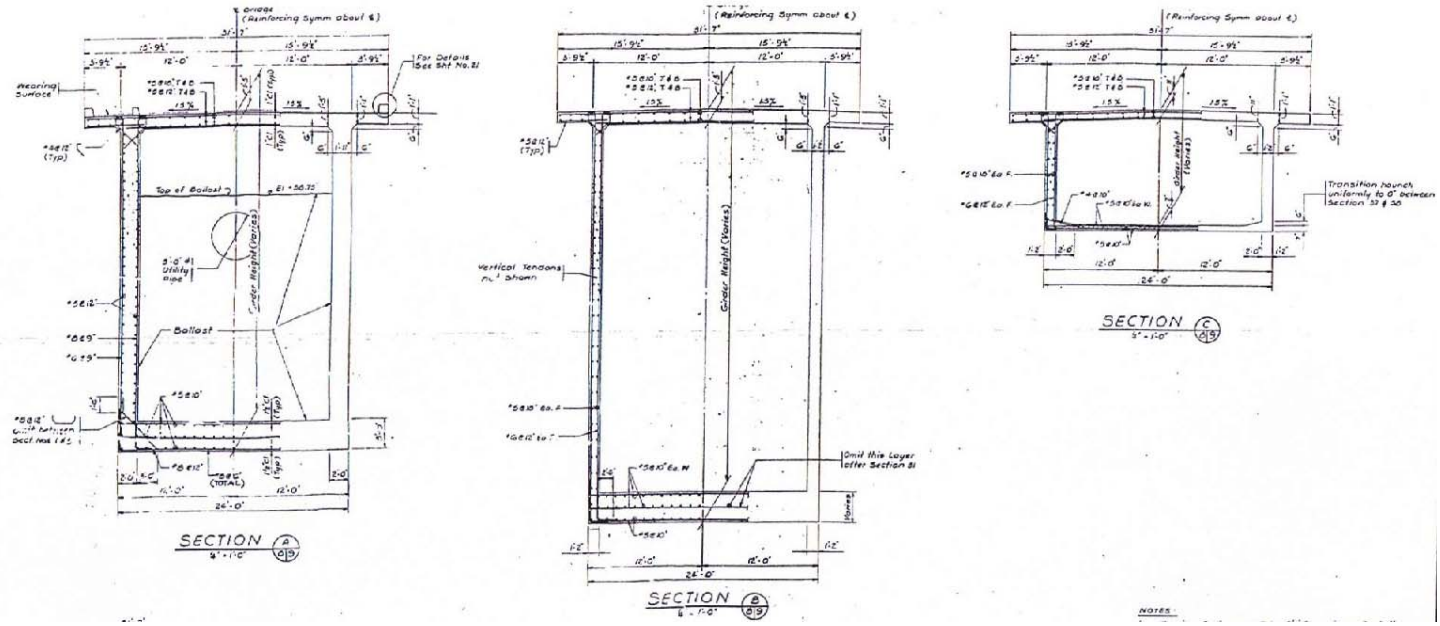

Fig. 2

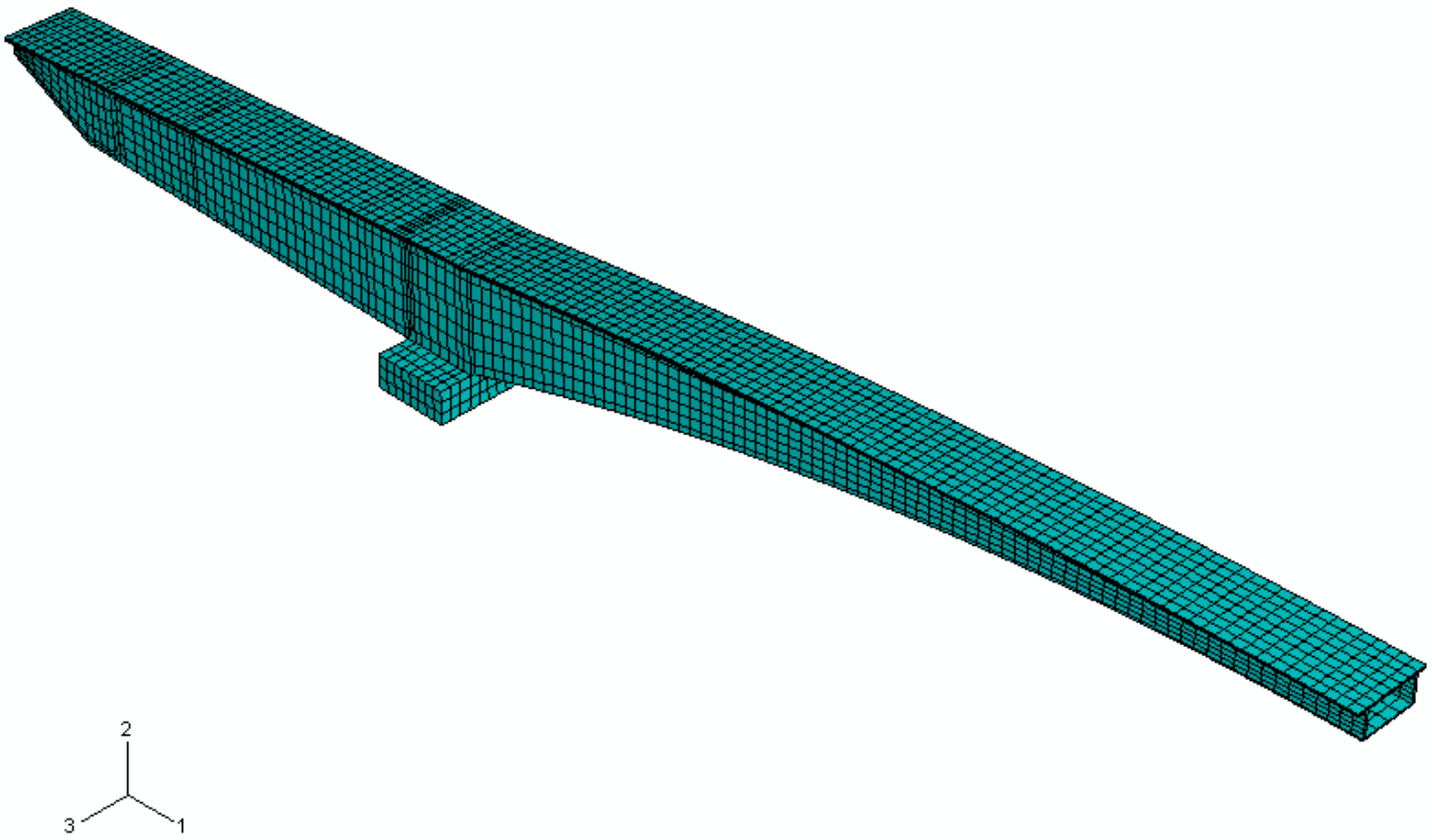

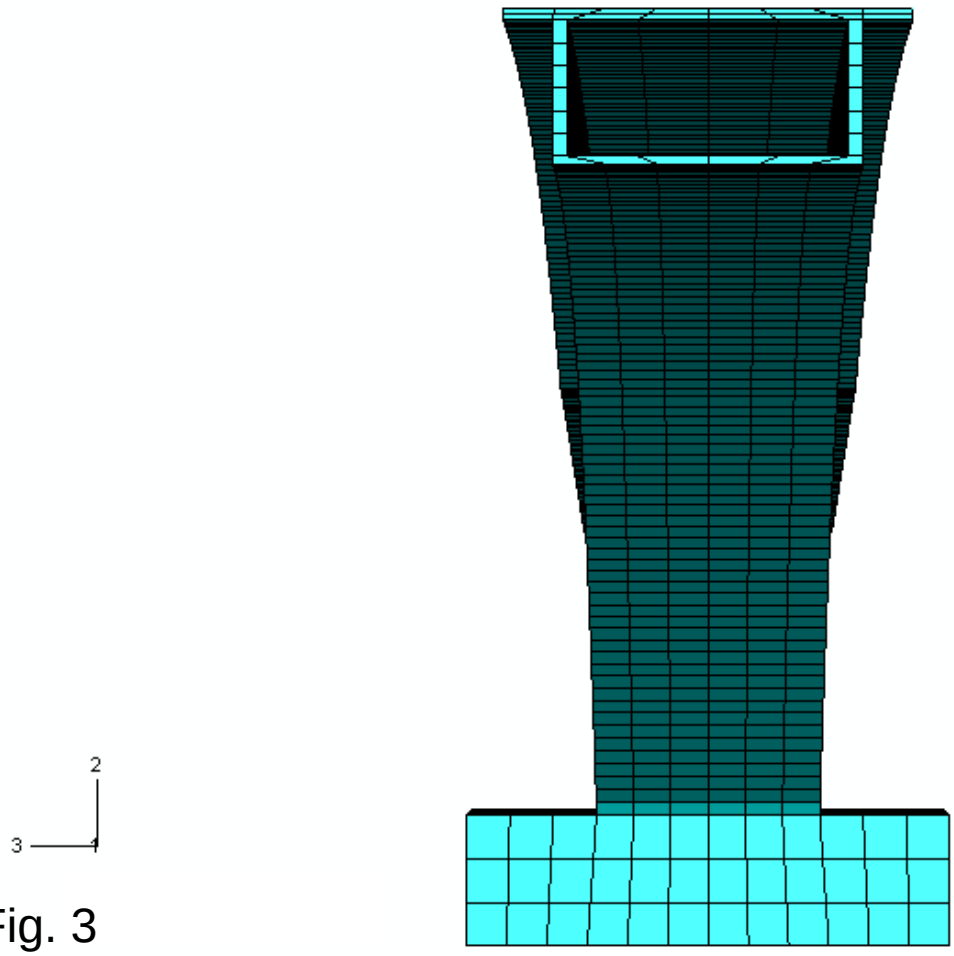

Fig. 3

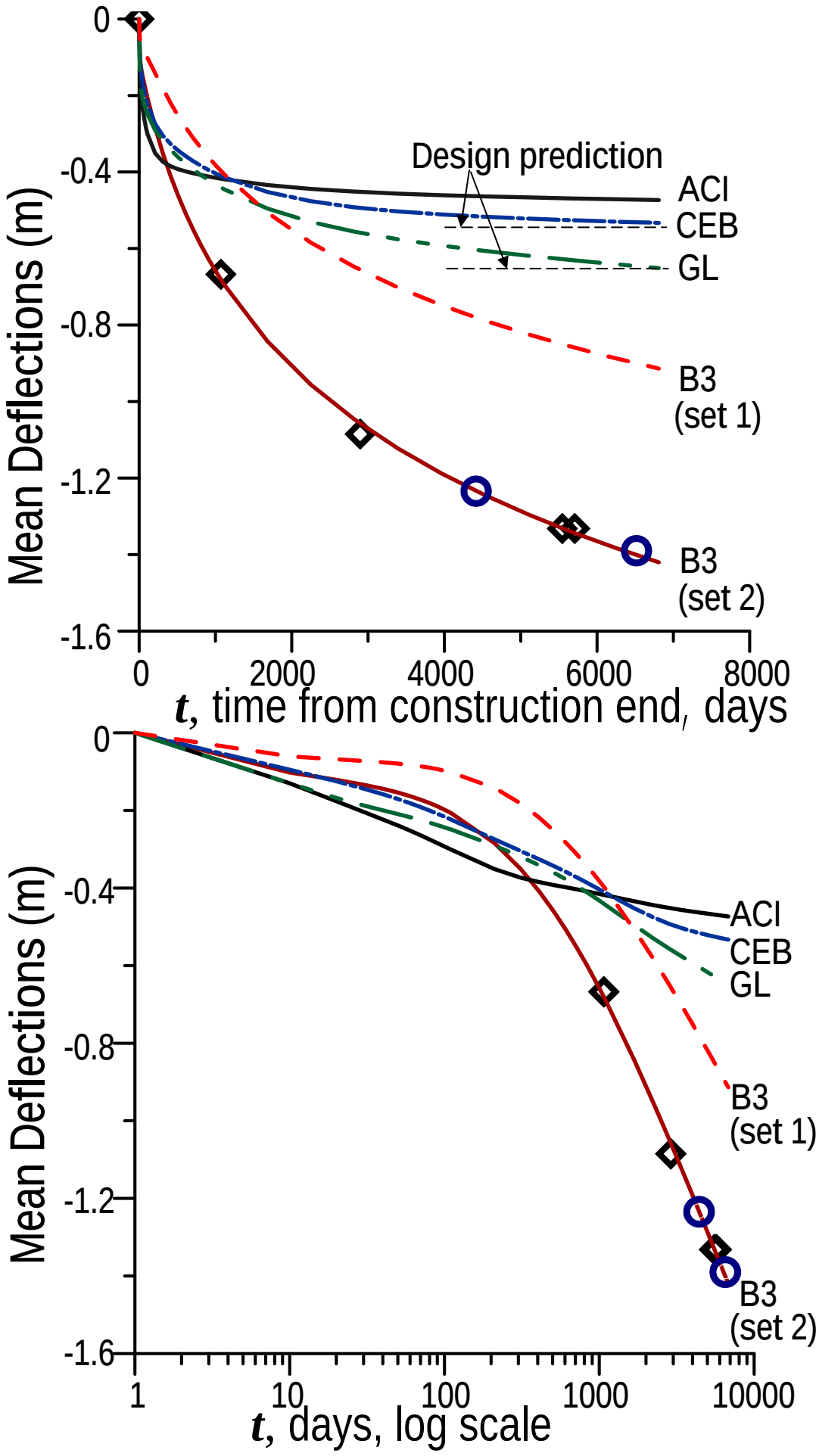
0
-0.4
-0.8
-1.2
-1.6
Mean Deflections (m)
Design prediction
ACI
CEB
GL
B3
(set 1)
B3
(set 2)
0
2000
4000
6000
8000
t, time from construction end, days
0
-0.4
-0.8
-1.2
-1.6
Mean Deflections (m)
ACI
CEB
GL
B3
(set 1)
B3
(set 2)
1
10
100
1000
10000
t, days, log scale

Fig. 4

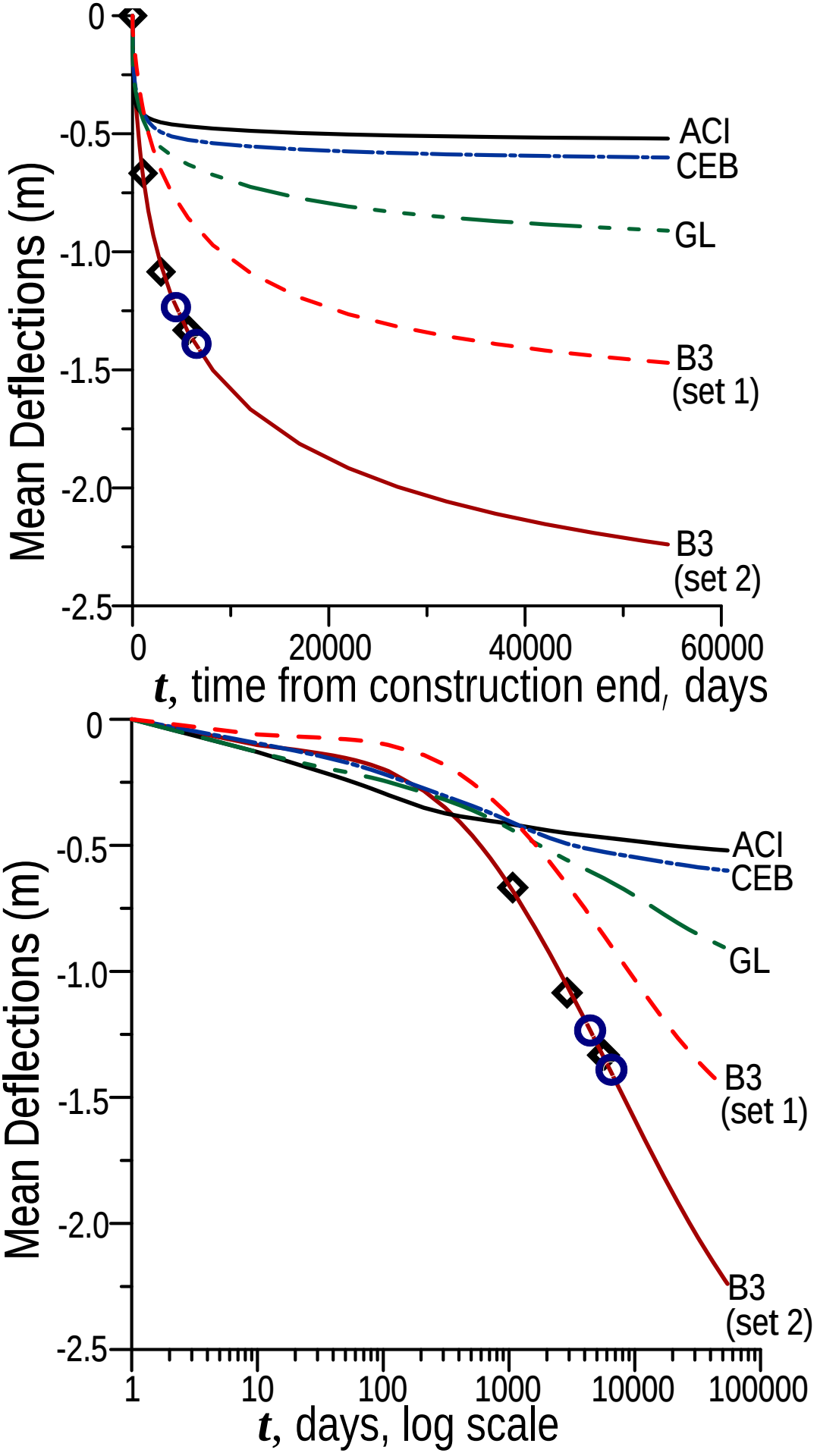
0
-0.5
-1.0
-1.5
-2.0
-2.5
Mean Deflections (m)
ACI
CEB
GL
B3
(set 1)
B3
(set 2)
0
20000
40000
60000
t, time from construction end, days
0
-0.5
-1.0
-1.5
-2.0
-2.5
Mean Deflections (m)
ACI
CEB
GL
B3
(set 1)
B3
(set 2)
1
10
100
1000
10000
100000
t, days, log scale

Fig. 5

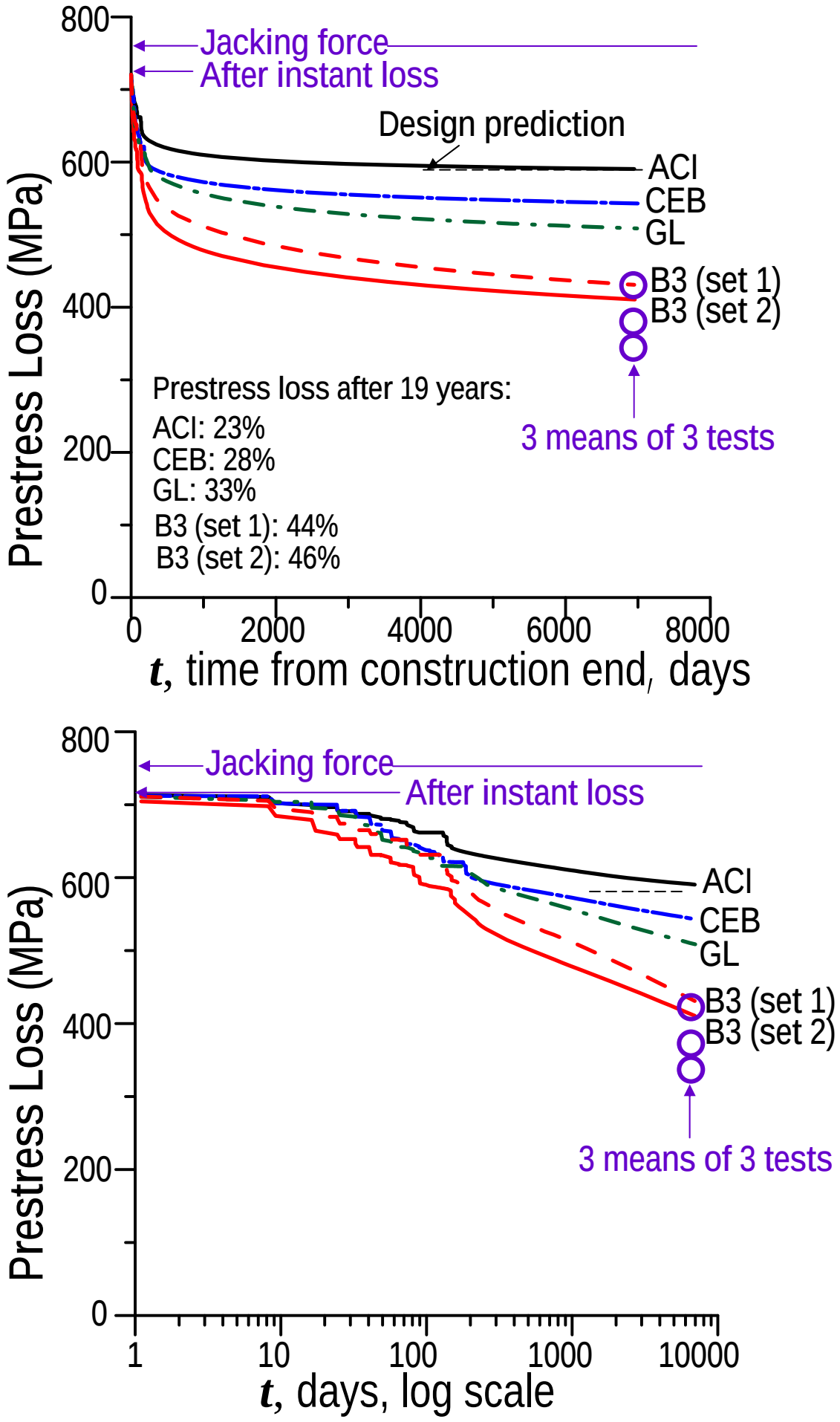
Jacking force
After instant loss
Design prediction
ACI
CEB
GL
B3 (set 1)
B3 (set 2)
3 means of 3 tests
Prestress loss after 19 years:
ACI: 23%
CEB: 28%
GL: 33%
B3 (set 1): 44%
B3 (set 2): 46%
Prestress Loss (MPa)
800
600
400
200
0
0
2000
4000
6000
8000
t, time from construction end, days
Jacking force
After instant loss
ACI
CEB
GL
B3 (set 1)
B3 (set 2)
3 means of 3 tests
Prestress Loss (MPa)
800
600
400
200
0
1
10
100
1000
10000
t, days, log scale

Fig. 6

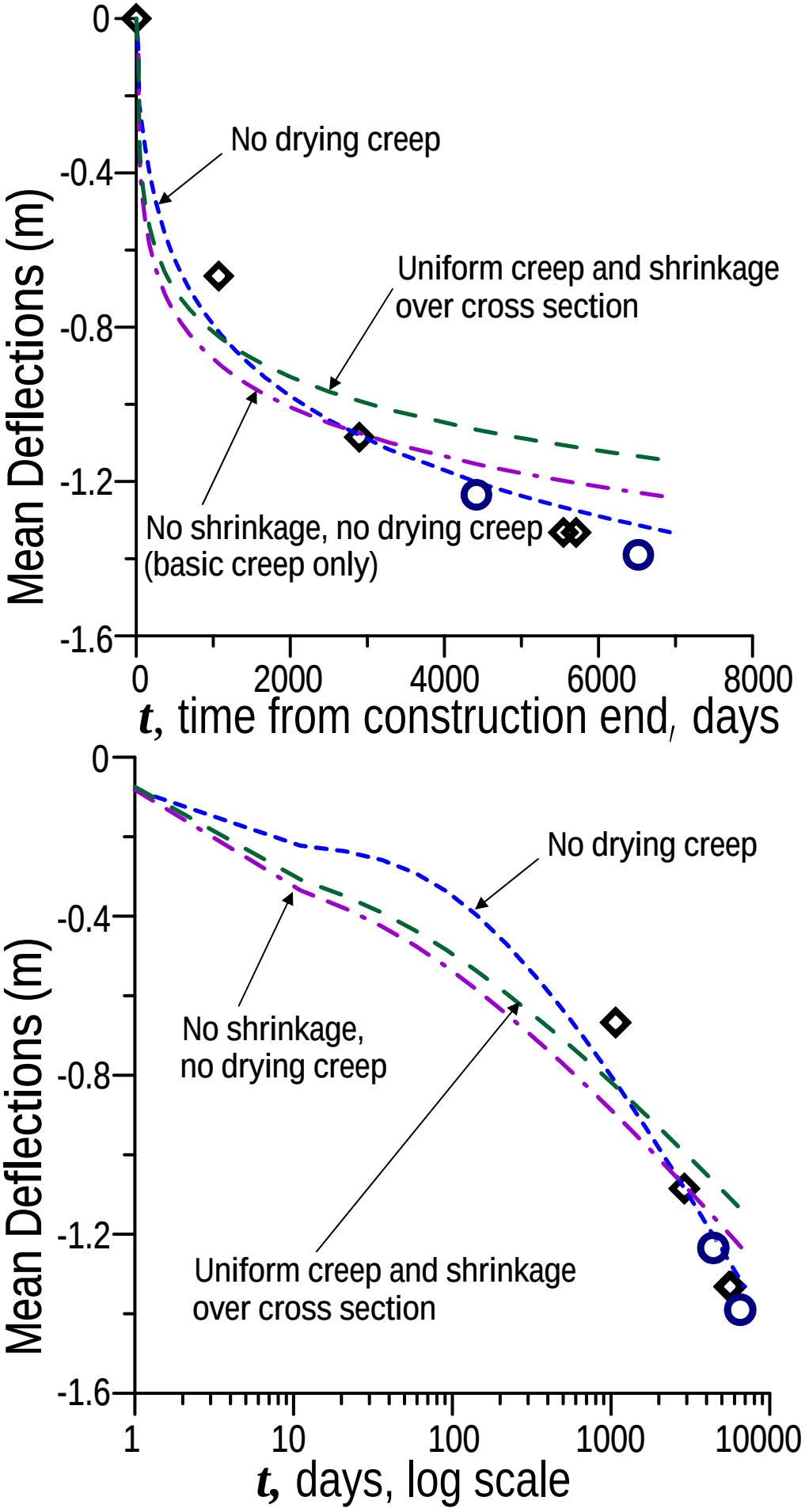
0
-0.4
-0.8
-1.2
-1.6
Mean Deflections (m)
No drying creep
Uniform creep and shrinkage
over cross section
No shrinkage, no drying creep
(basic creep only)
0
2000
4000
6000
8000
t, time from construction end, days
0
-0.4
-0.8
-1.2
-1.6
Mean Deflections (m)
No drying creep
No shrinkage,
no drying creep
Uniform creep and shrinkage
over cross section
1
10
100
1000
10000
t, days, log scale

Fig. 7

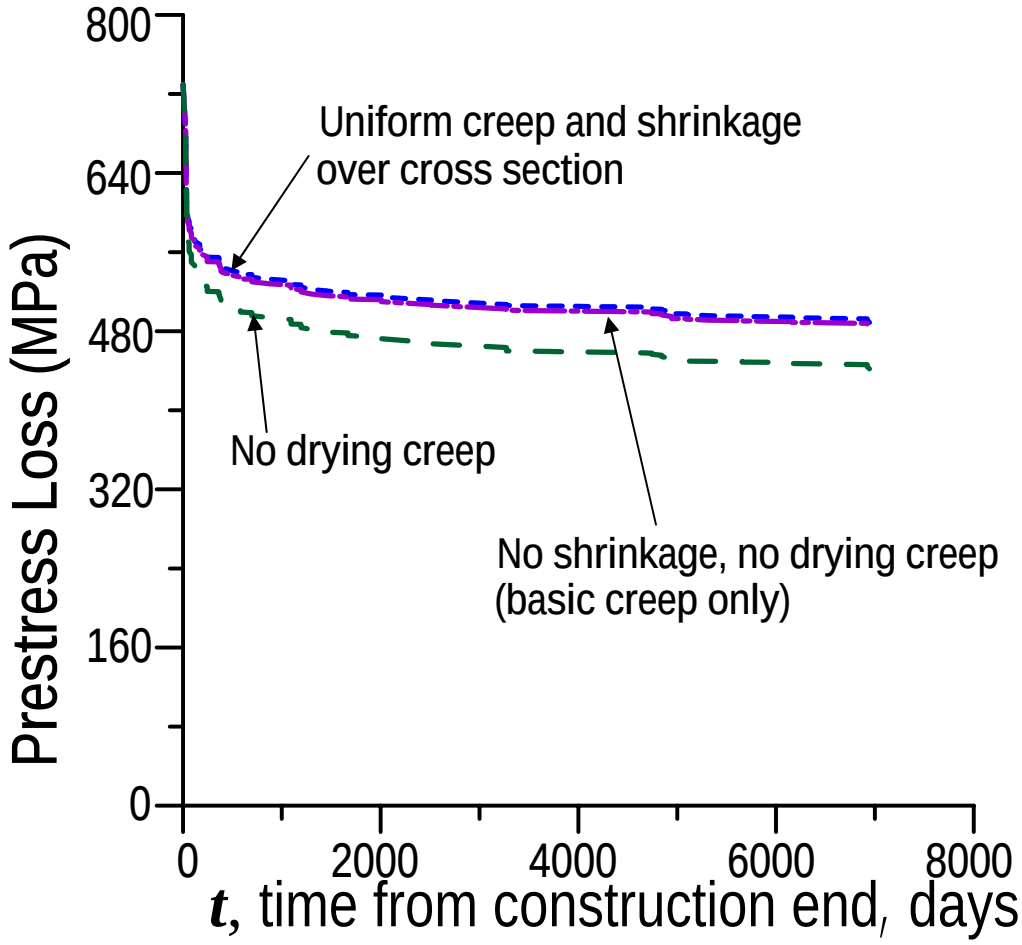
800
640
480
320
160
0
Prestress Loss (MPa)
Uniform creep and shrinkage
over cross section
No drying creep
No shrinkage, no drying creep
(basic creep only)
0
2000
4000
6000
8000
t, time from construction end, days

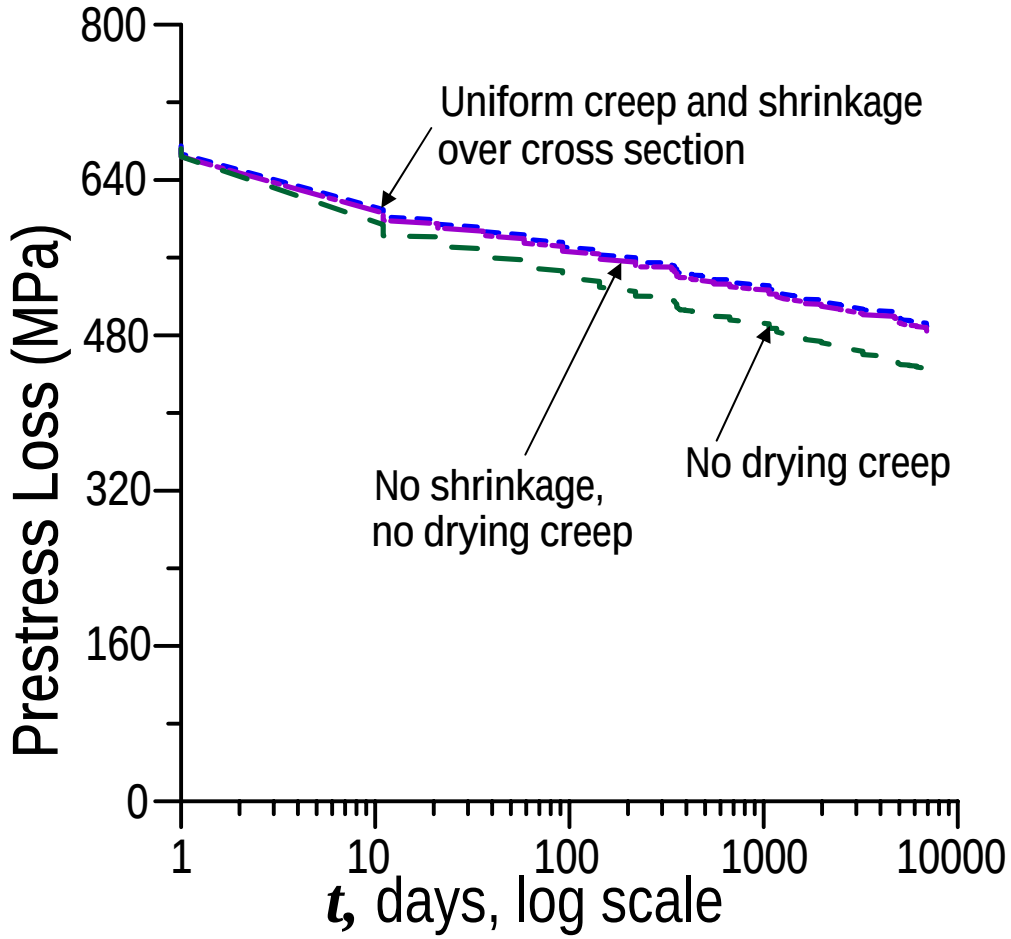
800
640
480
320
160
0
Prestress Loss (MPa)
Uniform creep and shrinkage
over cross section
No shrinkage,
no drying creep
No drying creep
1
10
100
1000
10000
t, days, log scale

Fig. 8

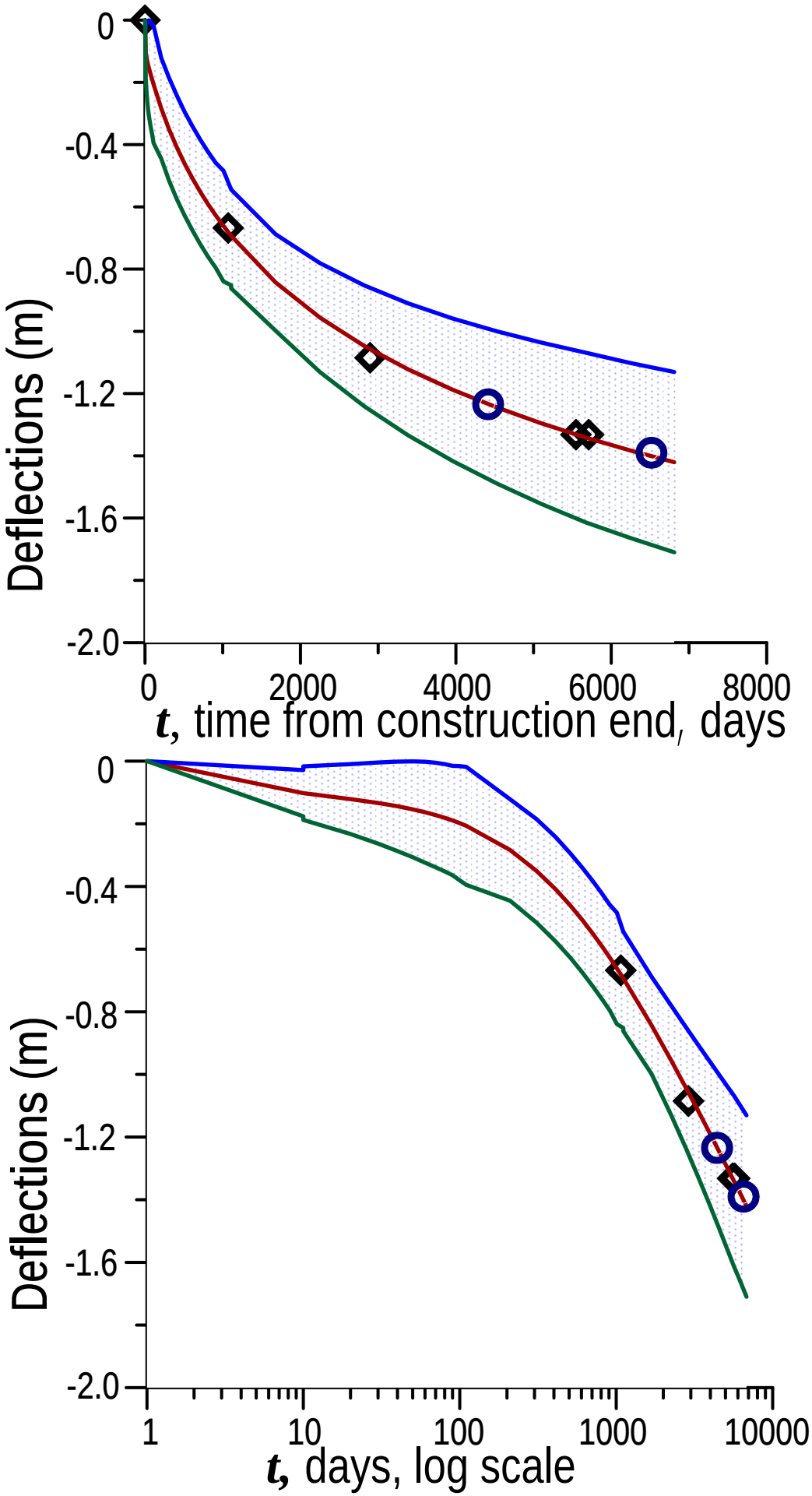
0
-0.4
-0.8
-1.2
-1.6
-2.0
Deflections (m)
0
2000
4000
6000
8000
t, time from construction end, days
0
-0.4
-0.8
-1.2
-1.6
-2.0
Deflections (m)
1
10
100
1000
10000
t, days, log scale

Fig. 9

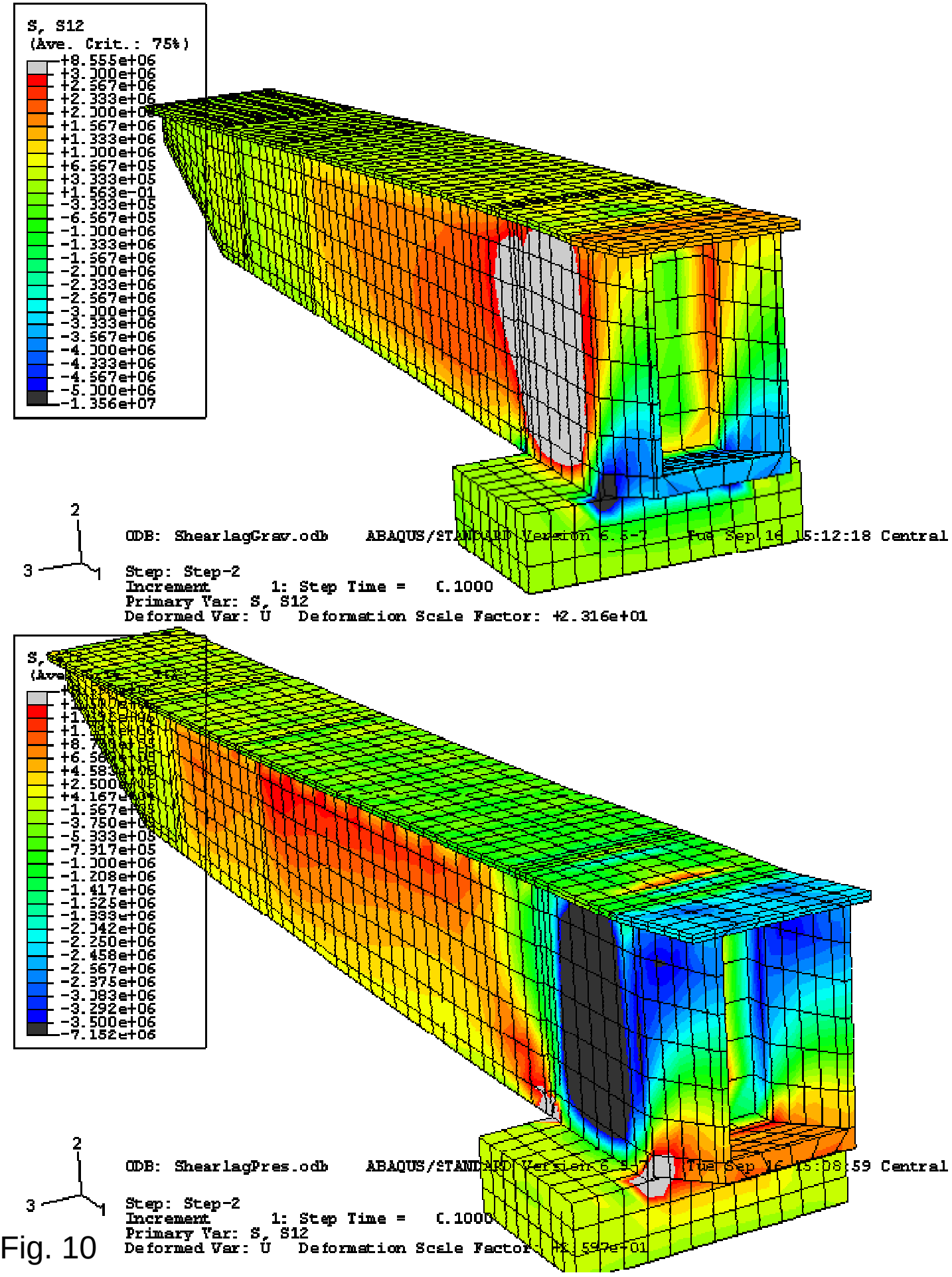
S, S12
(Ave. Crit.: 75%)
+8.555e+06
+3.000e+06
+2.567e+06
+2.333e+06
+2.000e+06
+1.567e+06
+1.333e+06
+1.000e+06
+6.567e+05
+3.333e+05
+1.563e-01
-3.333e+05
-6.567e+05
-1.000e+06
-1.333e+06
-1.567e+06
-2.000e+06
-2.333e+06
-2.567e+06
-3.000e+06
-3.333e+06
-3.567e+06
-4.000e+06
-4.333e+06
-4.567e+06
-5.000e+06
-1.356e+07
2
3
ODB: ShearlagGrav.odb ABAQUS/STANDARD Version 6.5-7 Tue Sep 16 15:12:18 Central
Step: Step-2
Increment 1: Step Time = 0.1000
Primary Var: S, S12
Deformed Var: U Deformation Scale Factor: +2.316e+01
S,
+1.000e+06
+6.567e+05
+4.583e+05
+2.500e+05
+4.167e+04
-1.567e+05
-3.750e+05
-5.333e+05
-7.917e+05
-1.000e+06
-1.208e+06
-1.417e+06
-1.525e+06
-1.833e+06
-2.042e+06
-2.250e+06
-2.458e+06
-2.567e+06
-2.875e+06
-3.083e+06
-3.292e+06
-3.500e+06
-7.152e+06
2
3
ODB: ShearlagPres.odb ABAQUS/STANDARD Version 6.5-7 Tue Sep 16 15:08:59 Central
Step: Step-2
Increment 1: Step Time = 0.1000
Primary Var: S, S12
Deformed Var: U Deformation Scale Factor: +2.597e+01

Fig. 10

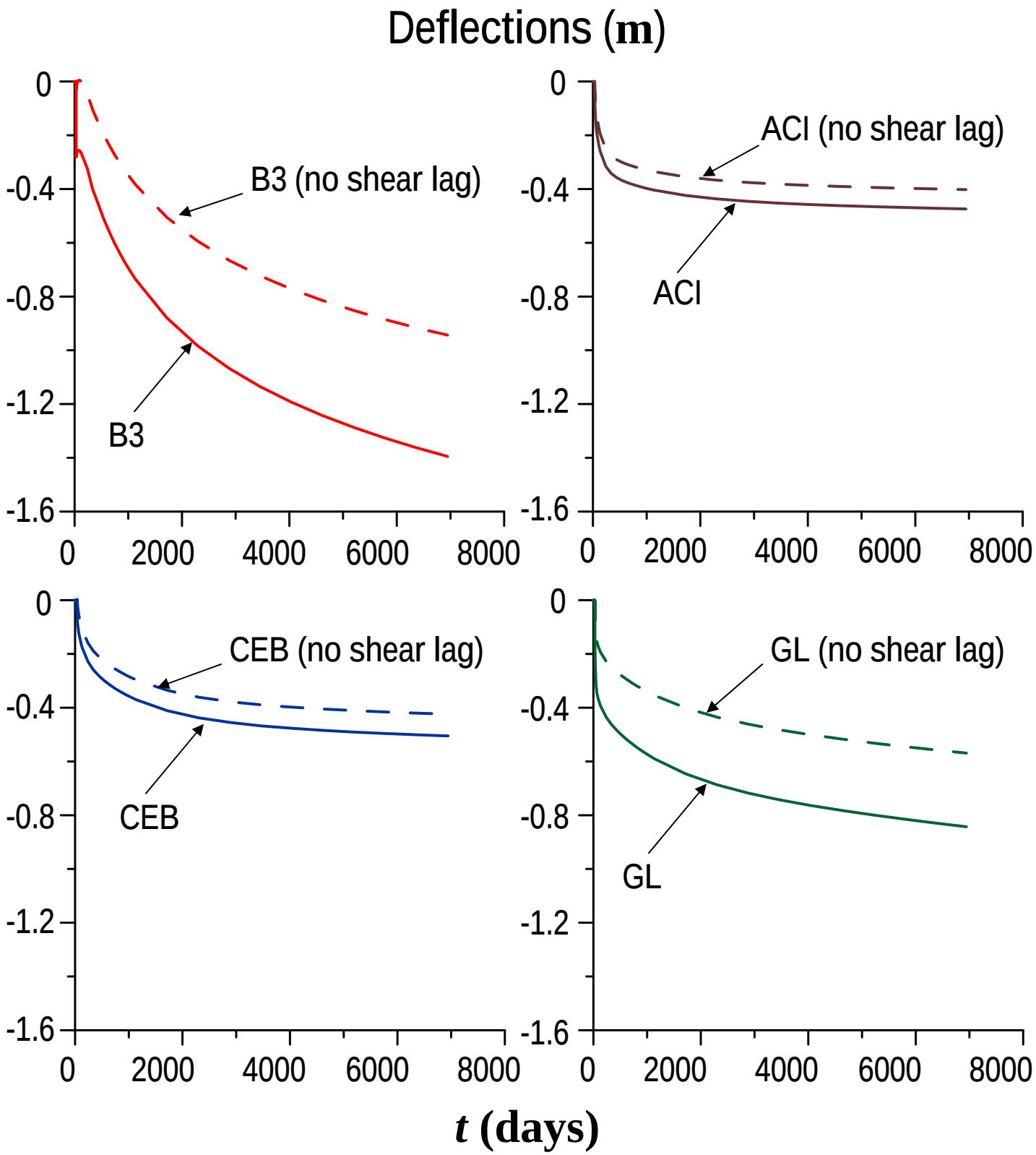
Deflections (m)
0
-0.4
-0.8
-1.2
-1.6
0
2000
4000
6000
8000
B3 (no shear lag)
B3
ACI (no shear lag)
ACI
CEB (no shear lag)
CEB
GL (no shear lag)
GL
t (days)

Fig. 11

Tsukiyono Bridge

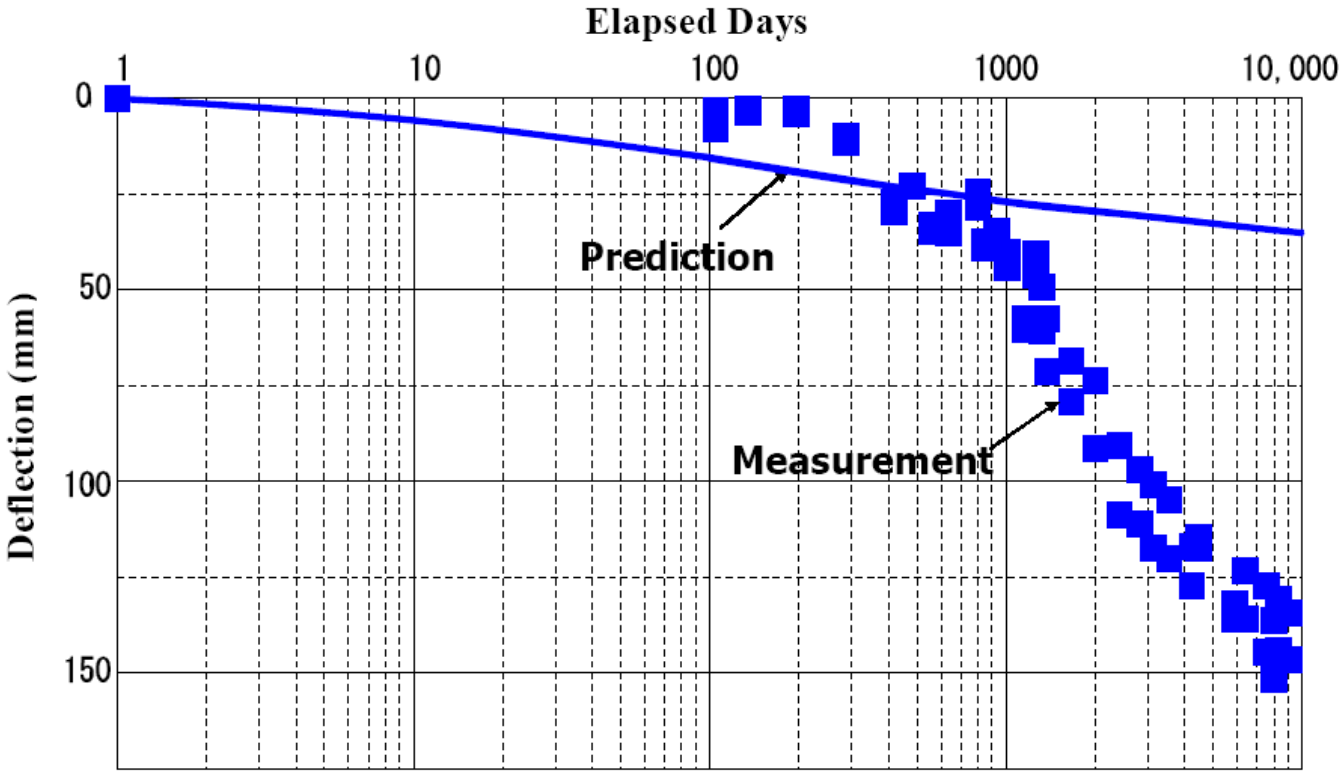

Fig. 12

Koshirazu Bridge

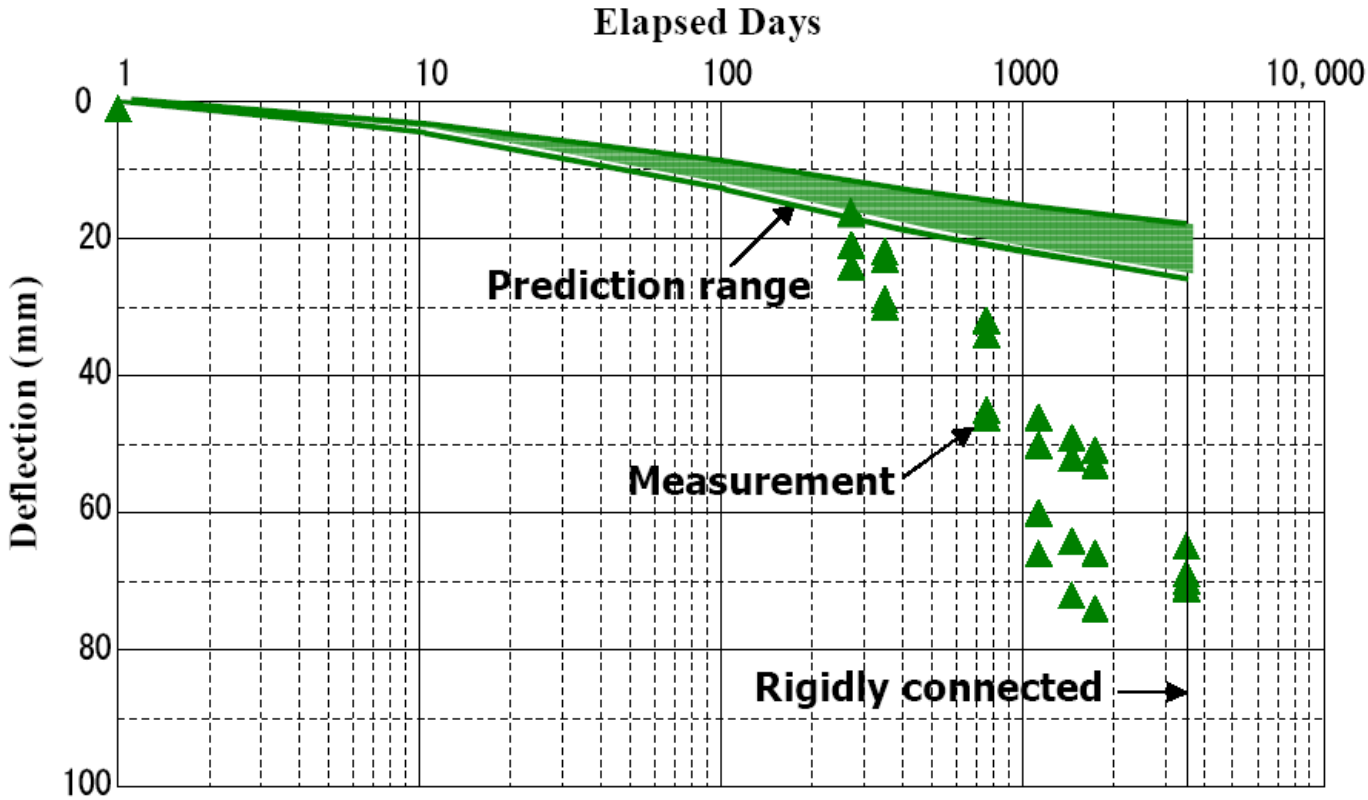

Fig. 13

Konaru Bridge

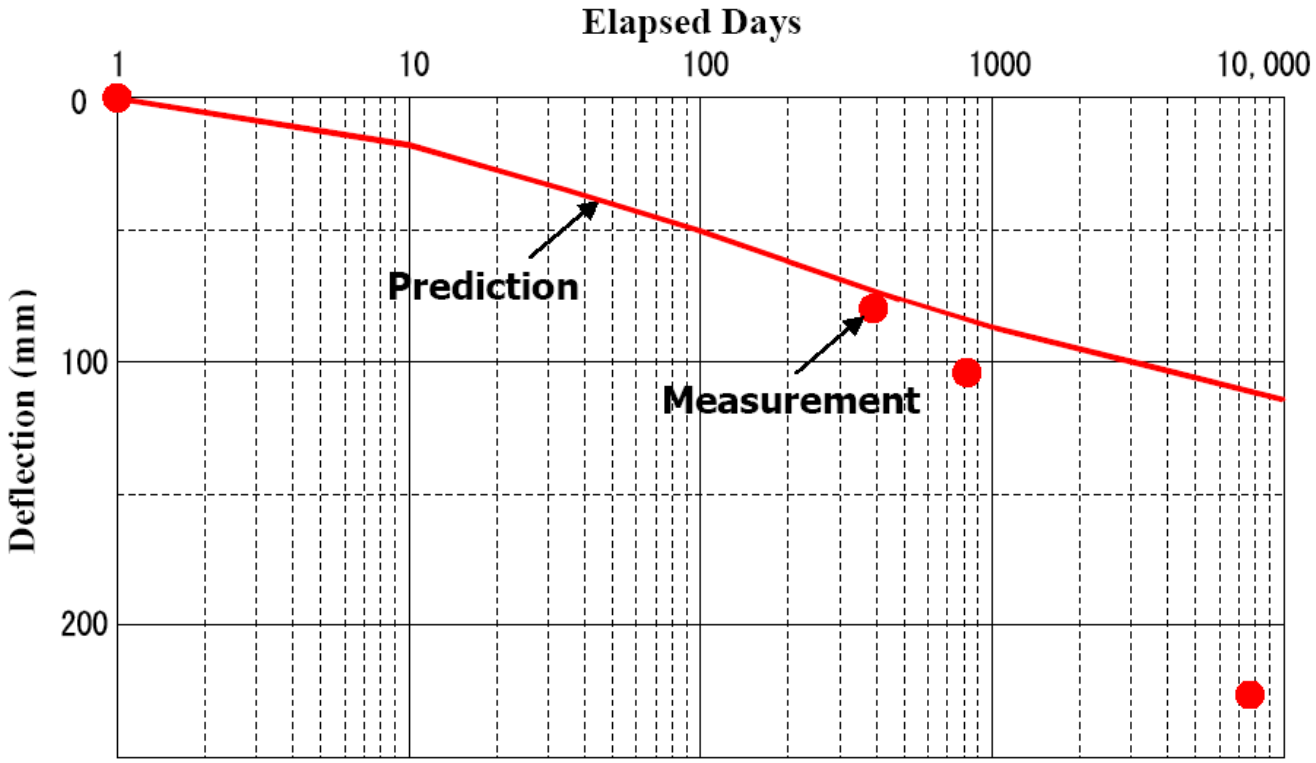

Fig. 14

Urado Bridge

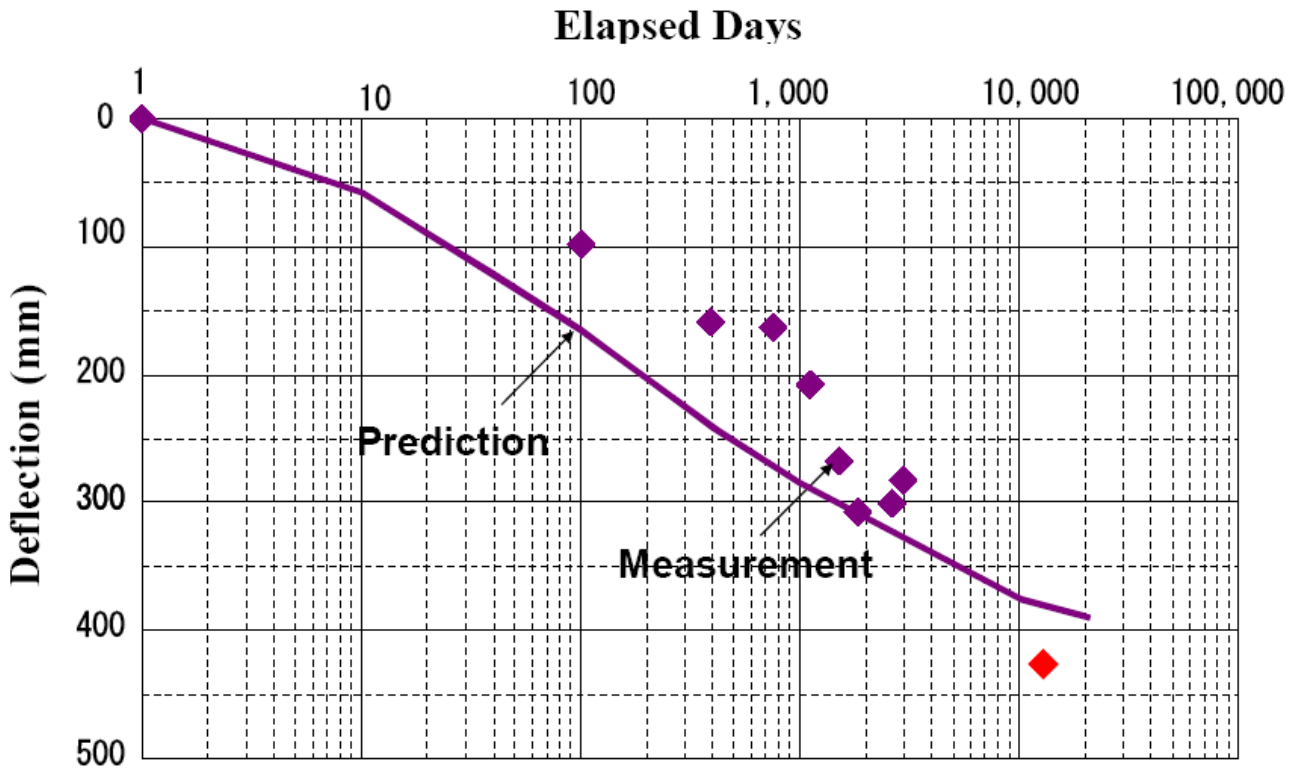

Fig. 15